Linköping Studies in Science and Technology
Dissertations No. 1445

Study of Six-Port Modulators and Demodulators for High-Speed Data Communications

Joakim Östh

Linköping University
INSTITUTE OF TECHNOLOGY

Department of Science and Technology
Linköping University, SE-601 74 Norrköping, Sweden

Norrköping 2012

Study of Six-Port Modulators and Demodulators for High-Speed Data Communications

Joakim Östh

A dissertation submitted to ITN, Department of Science and Technology, Linköping University, for the degree of Doctor of Technology.

ISBN: 978-91-7519-899-6
ISSN: 0345-7524
http://urn.kb.se/resolve?urn=urn:nbn:se:liu:diva-76087

Linköping University
Department of Science and Technology
SE-601 74 Norrköping
Sweden
Printed by LiU-Tryck, Linköping, Sweden, 2012.

Abstract

There is an increasing demand for high-speed wireless data communications to support consumers' need for, among other things, real time streaming of high definition video and fast file transfers. One radio architecture that has a potential to meet the increasing demand for high-speed data communications is a radio technique based on the six-port architecture. In addition to high-speed, the six-port radio also allows low power consumption and low cost. In this thesis, a comprehensive study of the six-port radio technique for high data rate ($>$ 1 Gbit/s) and low complexity are presented.

Firstly, a technique to suppress the carrier leakage was proposed, analyzed and verified by measurements. The proposed technique uses only a phase shifting network between the six-port correlator and its variable impedance loads, hence it is easy to implement. When the proposed carrier leakage suppression technique is used together with differential control signals, it also has the benefit of both improving the linearity and increasing the output power of the modulator. The same carrier leakage suppression technique can also be used in a six-port demodulator (receiver) to improve its performance.

Secondly, Schottky diodes were proposed to be used as high-speed variable impedance loads. A six-port modulator operating at 7.5 GHz, using the carrier leakage suppression technique together with Schottky diodes as variable impedance loads, was manufactured. Measurements on a 16 quadrature amplitude modulated (QAM) signal with a symbol rate of 300 Msymbol/s, i.e., a data rate of 1.2 Gbit/s, have proved high-speed operation, good modulation properties as well as carrier leakage suppression.

Thirdly, a six-port demodulator was built for high data rate applications and measurements were conducted to characterize its performance. De-

modulation of a 16-QAM signal at a data rate of 1.67 Gbit/s results in an acceptable bit error rate and error vector magnitude (EVM) performance.

Last but not least, new diode configurations were proposed, analyzed and verified for use in six-port demodulators. Using the proposed diode configurations, the use of differential amplifiers, as commonly used in a six-port demodulator, can be avoided. Avoiding the use of differential amplifiers allows high-speed processing and at the same time reduces the power consumption and implementation complexity. In the context of the new diode configurations, it was shown that a six-port receiver has better EVM vs frequency performance and lower implementation complexity, compared to a five-port or four-port receiver.

Populärvetenskaplig Sammanfattning

För dagens konsumenter är det en självklarhet att tillförlitligt kunna strömma video av hög kvalitet och att snabbt kunna överföra stora datamängder trådlöst. För att göra det möjligt krävs en radiolösning som kan hantera höga datahastigheter. En radioarkitektur som tillåter radiokommunikation med höga datahastigheter är en radio baserad på six-port tekniken. Six-port radioarkitekturen kan hantera höga datahastigheter samtidigt som en låg effektförbrukning och en låg kostnad bibehålls.

Denna avhandling summerar en omfattande studie av six-port tekniken för radiokommunikation med fokus på datahastigheter över 1 Gbit/s.

Först introduceras en ny teknik för att undertrycka bärvågsläckage (eng. carrier leakage) i en six-port modulator (sändare). Tekniken för att undertrycka bärvågsläckage använder sig av ett fasskiftande nätverk mellan six-port correlatorn och de varierbara impedanser som krävs för att skapa en modulerad radiofrekvens (RF) signal. Om tekniken för bärvågsundertryckning (eng. carrier leakage suppression) används tillsammans med differentiella kontrollsignaler till impedanserna, förbättras linjäriteten i modulatorn samtidigt som uteffekten fördubblas. Tekniken för bärvågsundertryckning kan med fördel även användas i en six-port demodulator (mottagare) för att göra den mindre känslig för bärvågsläckage och därmed förbättra demodulatorns prestanda.

För att verifiera tekniken för bärvågsundertryckning så tillverkades en prototyp. Six-port modulatorn designades för en center frekvens på 7.5 GHz. För att kunna hantera höga datahastigheter så använder six-port

modulatorn Schottky dioder som varierbara impedanser. Mätningar på en 16 quadrature amplitude modulated (QAM) signal vid 300 Msymbol/s, dvs en datahastighet på 1.2 Gbit/s verifierar dels att Schottky dioder tillåter höga datahastigheter och även att tillräcklig bärvågsundertryckning erhålls.

Även en six-port demodulator tillverkades för att karakterisera dess prestanda och potential. Mätningar har verifierat att demodulation av en 16-QAM modulerad signal med en datahastighet på 1.67 Gbit/s kan åstadkommas.

Nya diod konfigurationer för användning i six-port demodulator introducerades. Genom att använda de föreslagna diod konfigurationerna så kan basbands signalen återskapas utan att systemet behöver några differentiella förstärkare. Genom att undvika differentiella förstärkare, vilket tidigare var nödvändigt, möjliggörs höga datahastigheter samtidigt som en låg effektförbrukning kan bibehållas.

I samband med de nya diod konfigurationerna så undersöktes implementationskomplexiteten och prestandan mellan en six-port, five-port och four-port mottagare. Bäst prestanda med avseende på error vector magnitude (EVM) som funktion av frekvens erhålls med en six-port mottagaren om den används tillsammans med de nya diod konfigurationerna. Dessutom har six-port mottagaren den minsta implementationskomplexiteten.

Acknowledgments

First of all I want to thank my supervisor Professor Shaofang Gong and my co-supervisor Dr. Magnus Karlsson. I am grateful for their support. Both of them have contributed with important feedback, discussion and guidance during the research work.

I greatly appreciate the close co-operation and technical discussions with Dr. Owais.

Gustav Knutsson who has helped me with manufacture and assembly of prototypes is greatly appreciated.

Dr. Adriana Serban is acknowledged for useful discussions and support.

I also want to thank all members in the Communication Electronics Group for supporting my work.

Dr. Jaap Haartsen and Dr. Peter Karlsson at Sony Ericsson Mobile Communications AB are acknowledged for useful comments and suggestions.

Sony Ericsson Mobile Communications AB and Vinnova in Sweden are acknowledged for partial financial-support of this study.

Last but not least, I want to thank my parents Ove Östh and Agneta Östh, and my sister Maria Östh for encouragement and support.

Joakim Östh
Norrköping, May 2012.

List of Publications

The research work compiled in this dissertation was conducted in the Communication Electronics research group at the department of Science and Technology (ITN), Linköping University during the period from Nov 2008 to May 2012. It includes the following publications:

1. **J. Östh**, Owais, M. Karlsson, A. Serban, S. Gong, and P. Karlsson, "Direct carrier six-port modulator using a technique to suppress carrier leakage," *IEEE Transactions on Microwave Theory and Techniques*, vol. 59, no. 3, pp. 741–747, 2011.

2. **J. Östh**, M. Karlsson, A. Serban, and S. Gong, "Carrier Leakage Suppression and EVM Dependence on Phase Shifting Network in Six-Port Modulator," Accepted for presentation at *Proc. Int. Conf. Microwave and Millimeter Wave Technology (ICMMT 2012)*.

3. **J. Östh**, Owais, M. Karlsson, A. Serban, and S. Gong, "Schottky diode as high-speed variable impedance load in six-port modulators," in *Proc. IEEE Int Ultra-Wideband (ICUWB) Conf*, 2011, pp. 68–71.

4. **J. Östh**, A. Serban, Owais, M. Karlsson, S. Gong, J. Haartsen, and P. Karlsson, "Six-port gigabit demodulator," *IEEE Transactions on Microwave Theory and Techniques*, vol. 59, no. 1, pp. 125–131, 2011.

5. **J. Östh**, A. Serban, Owais , M. Karlsson, S. Gong, J. Haartsen, and P. Karlsson, "Diode configurations in six-port receivers with simplified interface to amplifier and filter," in *Proc. IEEE Int Ultra-Wideband (ICUWB) Conf*, vol. 1, 2010, pp. 1–4.

6. **J. Östh**, Owais, M. Karlsson, A. Serban, and S. Gong, "Performance evaluation of six-port receivers with simplified interface to amplifier and filter," in *Proc. IEEE Int Ultra-Wideband (ICUWB) Conf*, 2011, pp. 190–194.

7. **J. Östh**, Owais, M. Karlsson, A. Serban, and S. Gong, "Data and carrier interleaving in six-port receivers for increased data rate," in *Proc. IEEE Int Ultra-Wideband (ICUWB) Conf*, vol. 1, 2010, pp. 1–4.

8. **J. Östh**, M. Karlsson, Owais, A. Serban, and S. Gong, "Baseband Complexity Comparison of Six-, Five- and Four-Port Receivers," *Microwave and Optical Technology Letters*, vol. 54, no. 6, pp. 1502–1506, 2012.

9. **J. Östh**, A. Serban, M. Karlsson, and S. Gong, "LO Leakage in Six-Port Modulators and Demodulators and its Suppression Techniques," Accepted for presentation at *Proc. IEEE MTT-S Int. Microwave Symp. (IMS 2012).*

Papers published but not included in the dissertation:

1. Owais, **J. Östh**, A. Serban, M. Karlsson, and S. Gong, "Differential six-port demodulator," *Microwave and Optical Technology Letters*, vol. 53, no. 9, pp. 2192–2197, 2011.

2. Owais, **J. Östh**, and S. Gong, "Differential six-port modulator," in *Proc. Int Wireless Communications and Signal Processing (WCSP) Conf*, 2011, pp. 1–4.

3. A. Serban, **J. Östh**, Owais, M. Karlsson, S. Gong, J. Haartsen, and P. Karlsson, "Six-port transceiver for 6-9 ghz ultrawideband systems," *Microwave and Optical Technology Letters*, vol. 52, no. 3, pp. 740–746, 2010.

4. M. Karlsson, **J. Östh**, Owais, A. Serban, and S. Gong, "Circular dipole antennas for lower and upper uwb bands with integrated balun," in *Proc. IEEE Int. Conf. Ultra-Wideband ICUWB 2009*, 2009, pp. 658–663.

5. M. Karlsson, A. Serban, **J. Östh**, Owais, and S. Gong, "Frequency Triplexer for Ultra-wideband Systems (6-9 GHz)," Accepted for publication in *IEEE Transactions on Circuits and Systems I (IEEE TCAS-I).*

6. M. Karlsson, Owais, **J. Östh**, A. Serban, S. Gong, M. Jobs, and M. Gruden, "Dipole antenna with integrated balun for ultra-wideband radio 6-9 ghz," *Microwave and Optical Technology Letters*, vol. 53, no. 1, pp. 180–184, 2011.

7. A. Serban, M. Karlsson, **J. Östh**, O. Owais, and S. Gong, "Differential Circuit Technique for Six-Port Modulator and Demodulator," Accepted for presentation at *Proc. IEEE MTT-S Int. Microwave Symp. (IMS 2012).*

8. S. Gong, M. Karlsson, A. Serban, **J. Östh**, Owais, J. Haart- sen, and P. Karlsson, "Radio architecture for parallel processing of extremely high speed data," in *Proc. IEEE Int. Conf. Ultra-Wideband ICUWB*, 2009, pp. 433–437.

9. S. Gong, A. Huynh, M. Karlsson, A. Serban, Owais, and **J. Östh**, "Truly differential rf and microwave front-end design," in *Proc. IEEE 11th Annual Wireless and Microwave Technology Conf. (WAMICON),* 2010, pp. 1–5.

List of Abbreviations

ADC	Analog to Digital Converter
BPF	Band-Pass Filter
DCR	Direct Conversion Receiver
EVM	Error Vector Magnitude
HD	High Definition
I	In-Phase
LNA	Low-Noise Amplifier
LO	Local Oscillator
LPF	Low-Pass Filter
PA	Power Amplifier
PD	Power Detector
Q	Quadrature-Phase
QAM	Quadrature Amplitude Modulation
RF	Radio Frequency
TL	Transmission Line

Contents

1 Introduction

In today's world more and more devices become connected to the Internet to allow for global information exchange between users and/or machines. Another key factor is that the devices should not only be connected to Internet but also be mobile. Well known examples are mobile phones, smart phones and laptops. To allow for mobility the devices use wireless connection to the Internet. The data rate requirements on the wireless connections increase constantly. The high data rate is required to support, among other things, the user's need to allow for real time streaming of high definition (HD) video and fast file transfers. The radio systems must not only support high data rate, but also have a low cost and low power consumption to be attractive for device manufactures. The following three key parameters:

1. High data rate
2. Low cost
3. Low power consumption

must be considered when developing a new radio architecture suitable for the consumer market.

1.1 Background and Motivation

One relatively new and not so well known architecture to fulfill the requirements on high data rate (at least 1 Gbit/s), low cost and low power consumption is a radio based on the so called six-port technique. The core of a six-port radio, i.e., the six-port correlator, was first presented in 1964

by S. B. Cohn and N. P. Weinhouse [1]. At that time, the six-port correlator was used for microwave measurements. Much pioneer work for microwave measurements with the six-port correlator has been conducted by G. F. Engen and C. A. Hoer [2, 3]. The theory and use of a six-port correlator for measurements of scattering parameters have continued to evolve and are still an active area of research.

The idea to use the six-port correlator as a demodulator (receiver) was first presented by J. Li et al. in 1994 [4]. In 2005 the use of a six-port correlator for modulation was proposed by Y. Zhao et al. [5]. The use of a six-port correlator for modulation and demodulation has been well studied [4–28]. Among others, Professor Serioja Ovidiu Tatu, Ke Wu and Renato G. Bosisio are active in the six-port radio research and have contributed with major research results. However, for high-speed and ultra-wideband applications, there are still many problems to be solved.

1.2 Research Focus

The research focus of this work is divided into two main parts. The first part is the six-port based transmitter or modulator. The second part is the six-port based receiver or demodulator. Combining these two parts of transmitter and receiver allows for a complete transceiver system. The focus of this study is on modulator and demodulator so the power amplifier (PA) and low-noise amplifier (LNA) as well as antenna are not included.

The driving forces for the research in this thesis were to:

- Improve the performance to allow for high data rates, targeting 1 Gbit/s and beyond.
- Simplify the modulator/demodulator to reduce cost and/or power consumption.
- Identify and find solutions to overcome current limitations and drawbacks of the six-port radio architecture.

1.3 Outline of the Thesis

The thesis is of summary style and consists of a selected collection of the author's papers. However, to give a complete and clear picture of the six-port technique for modulators and demodulators and its relation to conventional techniques, the following additional chapters are included:

Chapter 2: *Six-Port Radio Background* - An introduction to the six-port technique for communications. Describes the principle and basic theory to understand how the six-port based demodulator and modulator operate. Differences between six-port radio and conventional mixer based radio are also discussed.

Chapter 3: *Six-Port Modulators in This Study* - The use of the six-port correlator together with variable impedance loads to generate a modulated RF signal from baseband I and Q data is described and analyzed. The problem with carrier leakage is identified and a solution is presented.

Chapter 4: *Six-Port Demodulators in This Study* - The use of the six-port correlator together with power detectors to recover the baseband I and Q data is described and analyzed. Improvements in the six-port demodulator architecture for improved performance is proposed, described and analyzed.

Chapter 5: *Own Contributions and Future Work* - Summarizes my contributions in the included papers and discusses potential future work.

2 Six-Port Radio Background

In this chapter the theory and operation principles of the six-port correlator, modulator and demodulator are described.

2.1 Six-Port Correlator

The six-port correlator is a passive device. Its phase difference between different ports are multiples of 90°, which allows orthogonal processing, i.e., to separate In-phase (I) and Quadrature-phase (Q) channels. The six-port correlator was first used in reflection coefficient measurements, but later its use as a communication device has been studied in [10]. Since then there has been much interest in the six-port correlator for communications [4–28].

2.1.1 Theory of Six-Port Correlator

A common configuration of a six-port correlator is shown in Fig. 2.1. The

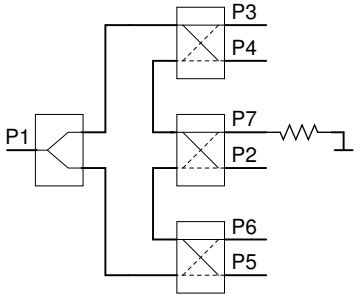

Fig. 2.1: Schematic of six-port correlator.

properties of this six-port correlator can directly be derived from its building blocks, i.e., the Wilkinson power divider and the three 90° hybrid couplers. Owing to the properties of the building blocks, an integer multiple of phase differences of 90° is presented between its ports. The same six-port correlator allows separation of I and Q channels in a six-port demodulator (receiver) and generation of a modulated radio frequency (RF) containing I and Q data in a six-port modulator (transmitter). In both the demodulator and modulator, only a single local oscillator (LO) source is required. The complete S-parameter matrix for the six-port correlator can be found by inspection of Fig. 2.1:

$$\mathbf{S} = \frac{1}{2}\begin{bmatrix} 0 & 0 & -1 & j & -1 & j \\ 0 & 0 & 1 & j & j & -1 \\ -1 & 1 & 0 & 0 & 0 & 0 \\ j & j & 0 & 0 & 0 & 0 \\ -1 & j & 0 & 0 & 0 & 0 \\ j & -1 & 0 & 0 & 0 & 0 \end{bmatrix} \tag{2.1}$$

with the relation between the incident waves $\mathbf{a}$ and reflected waves $\mathbf{b}$ (where $\boldsymbol{a}$ and $\boldsymbol{b}$ are vectors) with respect to the six-port correlator, as follows:

$$\mathbf{b} = \mathbf{S}\mathbf{a} \tag{2.2}$$

The ideal six-port correlator behavior was modeled by (2.1) and (2.2), and will be used to derive and analyze the functionality of both the six-port modulator and six-port demodulator.

2.2 Six-Port Modulator

For modulation, the six-port correlator can be used together with variable impedance loads to generate the modulated RF signal [5, 16, 17, 29], see Fig. 2.2. The variable impedance loads are controlled by a baseband signal and are used to generate different reflection coefficients on the respective

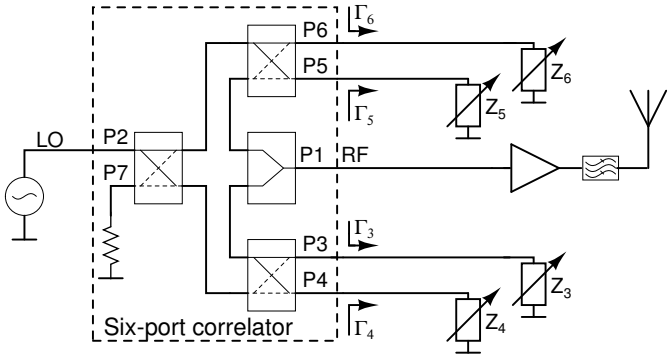

Fig. 2.2: Schematic of six-port modulator/transmitter.

ports on the six-port correlator. The variable reflection coefficients modulate an applied carrier signal. The variable impedance loads are usually implemented either by using switches [5, 17], transistors [15, 23, 29, 30] or diodes [20, 27].

Carrier leakage is a problem that is likely present when using variable impedance loads together with a six-port correlator for modulation [16, 23], and leakage degrades the performance of the transmitter-receiver chain [16, 31, 32]. To limit the effect of carrier leakage, balanced modulators can be used [29, 30, 33].

2.2.1 Building Blocks of Six-Port Modulator

The six-port modulator can be divided into two independent building blocks: the six-port correlator and the reflection coefficient generator. Combining these two blocks, the theory of the six-port modulator can be explained.

2.2.1.1 Six-Port Correlator

In a six-port modulator, as shown in Fig. 2.2, an LO source is connected to port P2 and generates an incident wave (a_2), this wave experiences different phase shifts and attenuations when it passes the six-port correlator to each

of the four output ports (P3 - P6). The transmitted or outgoing waves b_x on ports (P3 - P6) travel towards the impedance load Z_x where it gets reflected. The reflected waves are now at the input on ports (P3 - P6) and a part of it is transferred to the output port P1. Owing to the phase relations in the six-port correlator, and depending on how the impedance loads are selected, a modulated signal including both I and Q data can be generated. In an ideal six-port correlator, it is shown in Section 2.2.2 that the (complex) modulated output wave b_1 at port P1 is

$$b_1 = -\frac{a_2}{4}\left[(\Gamma_3 + \Gamma_4) + j\,(\Gamma_5 + \Gamma_6)\right] \tag{2.3}$$

where a_2 is the forward wave at port P2. Γ_3, Γ_4, Γ_5 and Γ_6 are the reflection coefficients at ports P3, P4, P5 and P6, as shown in Fig. 2.2. For modulation to occur, the value on Γ_3 - Γ_6 must change as a function of time.

2.2.1.2 Reflection Coefficient Generator

For generation of different reflection coefficients Γ_x, where $x \in \{3, 4, 5, 6\}$ is the port number, it is required to change the load impedance Z_x at ports (P3 - P6) as a function of a control voltage or baseband signal V_x. The reflection coefficient Γ_x is given by (2.4)

$$\Gamma_x\,(V_x) = \frac{Z_x\,(V_x) - Z_{0,x}}{Z_x\,(V_x) + Z_{0,x}} \tag{2.4}$$

where $Z_{0,x}$ is the characteristic impedance on the transmission line (TL) connecting impedance load Z_x to port Px on the six-port correlator. Observe that (2.4) is a nonlinear function of the impedance load.

2.2.2 Theory of Six-Port Modulator

To model the relation between the ports of the six-port correlator, S-parameters are used. The port numbers are defined as shown in Fig. 2.2. The output port for the modulated signal is defined to be P1, whereas P2 is defined

to be the input port for the carrier (LO). Ports P3 and P4 constitute one output port pair (P3, P4) and ports P5 and P6 the second output port pair (P5, P6). Define a reflection coefficient (Γ), incoming (a) and transmitted wave (b) on each of the ports P3, P4, P5 and P6

$$b_x = S_{x2} a_2 \tag{2.5}$$

$$a_x = \Gamma_x b_x \tag{2.6}$$

$$b_1 = S_{1x} a_x \tag{2.7}$$

The three main steps to get a modulated output signal are: a) the incoming wave is transferred from the input port (P2) to all the other ports in the six-port correlator resulting in the terms $b_x = S_{x2} a_2$, b) the transmitted wave b_x is reflected on the load impedance Z_x and gives an input wave at port Px, $a_x = \Gamma_x b_x$, and c) the input wave is transferred to the output port (P1), i.e., $b_1 = S_{1x} a_x = S_{1x} \Gamma_x S_{x2} a_2$. The total output wave is the sum of the reflections from each of the loads at port P3 - P6:

$$\begin{aligned} b_1 &= a_2 \sum_{x=3}^{6} S_{x2} \Gamma_x S_{1x} \\ &= a_2 \left(S_{32} \Gamma_3 S_{13} + S_{42} \Gamma_4 S_{14} + S_{52} \Gamma_5 S_{15} + S_{62} \Gamma_6 S_{16} \right). \end{aligned} \tag{2.8}$$

Using the ideal S-parameters as given in (2.1), it results in

$$b_1 = -\frac{a_2}{4} \left[(\Gamma_3 + \Gamma_4) + j \left(\Gamma_5 + \Gamma_6 \right) \right] \tag{2.9}$$

the value on the reflection coefficient Γ_x is in general complex. For modulation to occur, the value on Γ_x must change as a function of time. It is common that $\Gamma_3 = \Gamma_4$ and $\Gamma_5 = \Gamma_6$. If the reflection coefficient is approximated as a linear function of the applied baseband voltage $V = V_{CM} + \Delta v$

$$\Gamma(V) = \Gamma(V_{CM} + \Delta v) = \Gamma_{CM} + \Delta\Gamma \approx \Gamma_{CM} + \delta \Delta v \tag{2.10}$$

where $\Gamma_{CM} = \Gamma(V_{CM})$ is generated by the constant common mode voltage V_{CM}, and δ is the first derivative of Γ at V_{CM}, i.e.,

$$\delta = \frac{d\Gamma}{dV}|_{\Delta v=0} \tag{2.11}$$

and Δv the voltage deviation in the baseband signal that changes with time. Commonly the same type of impedance load is implemented on port pairs (P3, P4) and (P5, P6). If $\Gamma_3 = \Gamma_4 = \Gamma_I$ and $\Gamma_5 = \Gamma_6 = \Gamma_Q$ is used together with (2.9) and (2.10) then

$$b_1 = -\frac{a_2}{2}(\Gamma_I + j\Gamma_Q) = -\frac{a_2}{2}\left[\underbrace{\Gamma_{CM}(1+j)}_{\text{Carrier leakage}} + \underbrace{\delta(\Delta v_I + j\Delta v_Q)}_{\text{RF Modulated}}\right] \tag{2.12}$$

it is evident from (2.12) that only a part of the carrier signal a_2 is modulated to give the RF signal, whereas the other part gives an unwanted carrier leakage [20]. To avoid this leakage $\Gamma_{CM} = 0$ is required.

2.2.3 Six-Port Modulator Architectures

Two different configurations exist for the implementation of the six-port correlator for use in six-port modulators: a series or a parallel configuration [16]. The parallel configuration generally gives better modulation performance and hence most of the reported six-port modulators are based on the parallel configuration [5, 16, 17, 29]. The main difference between reported modulators is therefore found in terms of how the impedance loads are implemented and the modulation order they support. The three main types of impedance loads are:

- Switch matrices - vary the impedance in discrete steps.
- Transistors - vary the impedance in a continuous way by an analog control signal.
- Diodes - vary the impedance in a continuous way by an analog control signal.

Impedance loads implemented with switches posses a good linearity but, due to their limited speed, they are limited to low or moderate data rate applications [5,17]. Impedance loads implemented with transistors or diodes [15,23,27,29,30] allow high speed operation, but may have limited linearity.

A common problem with six-port based modulators is carrier leakage. The carrier leakage gives rise to, for example, unwanted in-band emission of the LO and degrades the performance in the receiver that in turn may decrease the channel capacity [34–36]. To decrease the impact of any present carrier leakage and to improve the modulation performance, balanced vector modulators have been proposed [29,30,33]. Unfortunately, their implementation requires several couplers and impedance loads, which results in increased system complexity.

2.3 Six-Port Demodulator

For demodulation, the six-port correlator can be used together with power detection, i.e., utilizing second-order nonlinearity, to recover the baseband signal [10,12,19,21,24], see Fig. 2.3. Schottky diodes are commonly used for power detection and allow high date rate due to their high-speed property. To recover the baseband signal the modulated RF and a coherent LO are applied to the six-port correlator. In other words, we are using the six-port demodulator in a direct conversion receiver. The phase relations in the six-port correlator together with the nonlinear processing allow to separate the I and Q baseband channels. The separated I and Q channels will, due to the nonlinear processing, not only contain the wanted baseband I and Q signals, but also a dc offset. It is well known that dc offset is a serious problem in a direct conversion receiver because the dc offset overlaps the wanted baseband signal [31,34]. However, by taking the difference between port pairs (P3, P4) and (P5, P6) the dc offset can be effectively suppressed in the detected baseband I and Q channels.

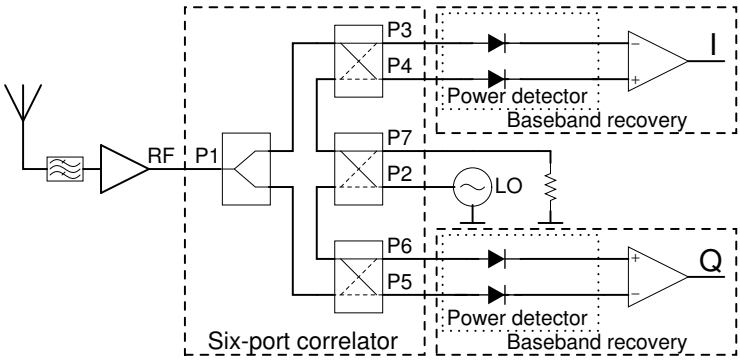

Fig. 2.3: Schematic of six-port receiver. The main building blocks are shown in rectangles, i.e., the six-port correlator, power detectors and baseband recovery circuit.

2.3.1 Building Blocks of Six-Port Demodulator

A six-port demodulator can be divided into three different building blocks: six-port correlator, power detection and baseband recovery. By combining all the three blocks, the theory for a complete demodulator is derived.

2.3.1.1 Six-Port Correlator

In a six-port receiver the six-port correlator (see Chapter 2.1) is used to linearly combine an LO signal with the modulated RF signal. The LO is assumed to be coherent with the RF signal (i.e., a direct conversion receiver). Using the circuit shown in Fig. 2.3, the modulated RF signal at port P1 and the LO signal at port P2 are combined with different phase shifts in the six-port correlator in accordance with the S-parameters of the six-port correlator, see (2.1). The output on ports P3 - P6 is input to a nonlinear device for power detection. A zero bias Schottky diode is commonly used for the power detection [10, 12, 19, 21, 24].

2.3.1.2 Power Detection

As previously mentioned a Schottky diode is usually used for the power detection, but any device with a (even-order) nonlinear characteristic can be used. The nonlinear transfer function of the diode will, among other frequencies, generate the demodulated baseband signal. A square law transfer function is used to model the current I_{PD} in an ideal power detector (PD) as a function of the applied voltage v.

$$I_{PD}(v) = kv^2 \tag{2.13}$$

where k is a constant.

2.3.1.3 Baseband Recovery

The outputs from the diode pairs at port (P3, P4) and port (P5, P6) are then fed to a differential baseband amplifier, as shown in Fig. 2.3. Taking the difference between the diode output current on specified ports results in I and Q data in two different paths, without any dc offset in the ideal case.

2.3.2 Theory of Six-Port Demodulator

The complete demodulation process with a six-port correlator is now derived [21, 37]. The modulated RF (z) and the LO (g) signals are described in the complex domain as follows:

$$z = A_{RF}(X_I + jX_Q)e^{j\omega t} \tag{2.14}$$

$$g = A_{LO}e^{j\phi}e^{j\omega t} \tag{2.15}$$

where ω is the angular frequency, ϕ is the relative phase between RF and LO, A_{LO} and A_{RF} are the LO and RF amplitudes, respectively. X_I and X_Q are the transmitted baseband I and Q data. The combined complex output on port Px on the six-port correlator due to the RF input on port P1 and

the LO input at port P2 is

$$y_x = S_{x2}g + S_{x1}z \tag{2.16}$$

where x corresponds to one of the four output ports P3 - P6, i.e., $x \in \{3, 4, 5, 6\}$, and S_{nm} is the S-parameter forward transmission from port m to port n of the six-port correlator. The incident wave on port P1 is therefore $a_1 = z$ and on port P2 it is $a_2 = g$. For modeling, an ideal power detector with a square law transfer function according to (2.13) is assumed. The real part of y_x:

$$Y_x = \Re\{y_x\} = \frac{y_x + \overline{y_x}}{2} \tag{2.17}$$

is used to calculate the time-domain signal. After power detection (squaring) and low-pass filtering (LPF) of the signal in (2.17), the time-domain output voltage V_x is given by:

$$V_x = \text{LPF}\left\{kY_x^2\right\} = k\frac{y_x\overline{y_x}}{2} = k\frac{|y_x|^2}{2} \tag{2.18}$$

Using (2.14) - (2.18) together with Euler's formula and setting $k = 1$ for simplicity results in, after some simplification, the following useful expression:

$$\begin{aligned} V_x \quad = \quad & |S_{x2}|^2 A_{LO}^2/2 + |S_{x1}|^2 A_{RF}^2 \left(X_I^2 + X_Q^2\right)/2 + \\ & A_{LO}A_{RF}|S_x|X_I \cos\left(\phi + \angle S_i\right) + \\ & A_{LO}A_{RF}|S_x|X_Q \sin\left(\phi + \angle S_i\right) \end{aligned} \tag{2.19}$$

where

$$|S_x| = |S_{x1}||S_{x2}| \tag{2.20}$$

$$\angle S_x = \angle S_{x2} - \angle S_{x1} \tag{2.21}$$

From (2.19) it is clear that the relative phase ϕ between the RF and LO signals as well as the phase and gain relations in the six-port correlator affect how much of X_I and X_Q that is present in the output signal V_x. Introducing

M_x, L_x, N_x and R to keep the notations shorter:

$$M_x = |S_{x2}|^2 A_{LO}^2/2 \tag{2.22}$$

$$L_x = |S_{x1}|^2 A_{RF}^2/2 \tag{2.23}$$

$$N_x = A_{LO} A_{RF} |S_x| \tag{2.24}$$

$$R = X_I^2 + X_Q^2 \tag{2.25}$$

then (2.19) may be expressed in matrix form

$$\underbrace{\begin{bmatrix} M_3 & L_3 & N_3\cos\angle S_3 & N_3\sin\angle S_3 \\ M_4 & L_4 & N_4\cos\angle S_4 & N_4\sin\angle S_4 \\ M_5 & L_5 & N_5\cos\angle S_5 & N_5\sin\angle S_5 \\ M_6 & L_6 & N_6\cos\angle S_6 & N_6\sin\angle S_6 \end{bmatrix}}_{\mathbf{D}} \begin{bmatrix} 1 \\ R \\ X_I \\ X_Q \end{bmatrix} = \begin{bmatrix} V_3 \\ V_4 \\ V_5 \\ V_6 \end{bmatrix} \tag{2.26}$$

This matrix model is used to describe the six-port demodulator. The matrix **D** is dependent on the actual implementation of the six-port correlator and directly related to the S-parameters of the six-port correlator. The LO power is assumed to be known in the demodulator and therefore only X_I, X_Q and R are unknown. The S-parameters for the ideal six-port correlator are given by:

$$\mathbf{S} = \frac{1}{2}\begin{bmatrix} 0 & 0 & -1 & j & -1 & j \\ 0 & 0 & 1 & j & j & -1 \\ -1 & 1 & 0 & 0 & 0 & 0 \\ j & j & 0 & 0 & 0 & 0 \\ -1 & j & 0 & 0 & 0 & 0 \\ j & -1 & 0 & 0 & 0 & 0 \end{bmatrix} \tag{2.27}$$

from which the **D** matrix can be derived from (2.22) - (2.26)

$$\mathbf{D} = \frac{1}{8}\begin{bmatrix} A_{LO}^2 & A_{RF}^2 & -2A_{LO}A_{RF} & 0 \\ A_{LO}^2 & A_{RF}^2 & 2A_{LO}A_{RF} & 0 \\ A_{LO}^2 & A_{RF}^2 & 0 & -2A_{LO}A_{RF} \\ A_{LO}^2 & A_{RF}^2 & 0 & 2A_{LO}A_{RF} \end{bmatrix} \tag{2.28}$$

There are only three unknown variables in this linear model: X_I, X_Q and R, but four equations are available, therefore one of the equations is linearly dependent on the others and **D** is singular. By inspection of (2.28) together with (2.26), it is seen that the detected I signal I_d (I channel) can be recovered by taking the difference of $V_4 - V_3$, and the detected Q signal Q_d (Q channel) by taking the difference of $V_6 - V_5$:

$$I_d = \frac{2}{A_{LO}A_{RF}}(V_4 - V_3) \tag{2.29}$$

$$Q_d = \frac{2}{A_{LO}A_{RF}}(V_6 - V_5) \tag{2.30}$$

Both the dc offset from LO (M_x) and the nonlinear distortion (R) are canceled on the I and Q channel outputs in this case. In an ideal system the detected I-Q symbols should be an exact scaled copy of the transmitted symbols, i.e., $I_d = kX_I$ and $Q_d = kX_Q$ where k is a scaling factor. In a realistic system there may be phase and/or amplitude imbalances in the six-port correlator and, therefore, crosstalk between I and Q channels.

2.3.3 Six-Port Demodulator Architectures

According to the derived theory of the six-port demodulator, to recover the baseband I and Q channels with dc offset suppression, equation (2.29) - (2.30) must be implemented.

2.3.3.1 Direct Sampling of the Power Detector Output

One approach is to first amplify and low-pass filter each of the four outputs from the power detectors [4, 14, 26] and then sample the output with an analog to digital converter (ADC) and implement (2.29) - (2.30) in the digital domain. In this configuration four baseband amplifiers, four filters and four ADCs are used. A challenge, if a ADC is used, to directly sample each of the four outputs of the power detectors is that they need to operate at high-speed to support high symbol rates. The high-speed operation required for the four ADCs increases the system cost and power consumption.

2.3.3.2 Using Differential Amplifier

Another approach is to use differential amplifiers [11,21,24,38] that are used to implement (2.29) - (2.30), i.e., to take the difference between port pairs to recover the baseband I and Q channels. In this case, the number of ADCs can be reduced from four to two. An analog decision circuit may also be implemented to directly demodulate the data without using any ADC or digital signal processing [15, 24, 39]. Depending on the modulation used, an analog decision circuit may be a good choice for high date rate applications.

2.4 Six-Port Radio vs Conventional Radio

In general, two main radio architectures exist, the heterodyne architecture and the direct conversion, or homodyne, architecture [31, 40]. Both have their respective pros and cons. The direct conversion architecture has gained increasing interest due to its simpler architecture. The six-port radio utilizes a direct conversion architecture. The equivalence between a conventional direct conversion radio using mixers and the six-port technique is clear from the previous theoretical discussion on six-port modulator and demodulator and has been proved in [18]. The key differences between six-port radio and conventional radio based on mixers are therefore presented in the context of a direct conversion architecture.

2.4.1 Reflection Based vs Mixer Based Modulator

As explained in Chapter 2.2, a six-port modulator generates the modulated RF signal directly from an LO source (carrier) in terms of the reflection coefficients at specific ports. The reflection coefficients are generated from variable impedance loads. Hence, if the impedance is controlled by a baseband signal, modulation is possible. This reflection based technique to generate a modulated signal is well known [30, 33, 41–43].

In a reflection based modulator (six-port), the baseband I and Q data control the reflection coefficient present at specific ports and the carrier wave is multiplied with these reflection coefficients to generate a modulated RF signal. In a mixer based modulator, the baseband I and Q channels are multiplied with the carrier by means of a mixer.

Because the six-port is a passive and linear device, the output power can be increased by increasing the LO power and the use of a PA can to some extent be avoided. A typical mixer, based on diodes or transistors, is certainly nonlinear and has therefore limited power handling capability. The reflection based modulation technique, that is used in a six-port modulator, can be used with spectral shaping, linearization and digital predistortion techniques. A modulated output signal with good properties in time and frequency domain can thus be generated [42].

2.4.2 Power Detection Based vs Mixer Based Demodulator

In a six-port demodulator recovery of I and Q baseband signals are done by using power detection at the four outputs of the six-port correlator. Owing to the relative phase differences between the four output ports, the two input waves, i.e., the RF and LO signals add constructively or destructively and this is detected by the power detector, commonly implemented with a Schottky diode [14, 18]. In a conventional mixer based direct conversion demodulator, two mixer cores, one for I channel and one for Q channel, are used. The mixers commonly operate in switching mode, so its conductance changes from a high to low state and thereby allows frequency conversion,

i.e., demodulation. In general switching mode mixers require more LO power than power detection.

2.4.3 Pros and Cons of the Six-Port Radio

The previous section has discussed key differences between six-port modulator/demodulator compared to a traditional direct conversion modulator/demodulator based on mixers. Performance evaluation on six-port radio as well as comparative studies between six-port radio and conventional mixer based radio can be found in the literatures [9, 11, 12, 24, 28, 44]. Based on these results, pros and cons of the six-port radio technique in comparison with a traditional direct conversion radio can be listed.

Pros:

- High bandwidth –> high data rate
- Passive circuit –> high linearity and low loss
- Power detection –> low power
- Six-port correlator is a distributed circuit –> scalable with frequency

Cons:

- Diode detectors –> low sensitivity
- Diode detectors –> limited dynamic range
- Six-port correlator is a distributed circuit –> large size at low frequency

2.5 Challenges Associated with Six-Port Radio

A six-port based modulator and demodulator, i.e., a six-port radio, share much of the properties and challenges that are known from direct conversion

modulators and demodulators. Hence, much of the challenges associated with six-port radio is similar to the challenges for direct conversion radios [34, 45, 46].

2.5.1 Dc Offset

The dc offset is a serious problem in a direct conversion receiver (DCR) and hence in the six-port demodulator. Because the wanted baseband signal as well as the unwanted dc offset both are centered at dc, they can not be separated by filtering. If the dc offset is severe, it may saturate the following baseband amplifiers.

The dc offset can be divided into two types: a) a static dc offset, and b) a dynamic dc offset. The static dc offset is assumed to be constant, or to change slowly and can relatively easily be compensated for. The dynamic dc offset is more problematic as it changes with time. Both types of dc offset will interfere with the baseband signal and degrade the receiver performance or, if the dc offset is severe, even saturate stages in the receiver chain. There are several mechanisms that can generate dc offset, such as LO leakage and LO self-mixing [34, 45, 46].

2.5.2 LO Leakage

Due to finite isolation from LO to RF port, a part of the LO signal reaches the RF port. This signal, i.e., the LO leakage or carrier leakage, gives rise to a number of problems:

- In a receiver, the LO leakage passes through the front end filter and amplifiers and reaches the antenna, where it is radiated. The radiated LO leakage may be reflected in the environment and received by the antenna and upon mixing with the LO, contributing to the LO self-mixing.
- In a receiver (demodulator), the LO leakage reaches the RF input of the LNA and if the signal level is too high, it saturates the LNA and/or

other blocks in the RF chain.

- In a modulator (transmitter) the LO leakage results in in-band LO radiation and decreased SNR.

These effects are clearly unwanted as it, among other things, contaminates the RF spectrum and degrades the performance of the receiver.

2.5.3 LO Self-Mixing

LO self-mixing is the case when a part of the LO signal reaches the RF input port and mixes with itself. Several paths exist, due to finite isolation between the RF and LO ports. A part of the LO reaches the RF port and upon reaching the band-pass filter (BPF), LNA and antenna a part of the LO leakage is reflected back towards the RF input port of the six-port demodulator and generates and unwanted dc signal at the output of the power detectors that may interfere with the baseband data.

3 Six-Port Modulators in This Study

For modulation, the six-port correlator can be used together with variable impedance loads (see Fig. 3.1) to generate the modulated RF signal, as discussed in Chapter 2.2. The use of variable impedance loads is known to create problem with carrier leakage [16, 23]. A new approach to suppress the carrier leakage is therefore presented and discussed in this study. The proposed solution to suppress the carrier leakage is further investigated in terms of its performance vs frequency and how it affects the modulation performance, in terms of the error vector magnitude (EVM). As the final step a Schottky diode as a high-speed variable impedance load is proposed and analyzed. The Schottky diode based impedance load, together with the carrier leakage suppression technique, allows for data rates above 1 Gbit/s with good modulation performance and suppressed carrier leakage.

3.1 Carrier Leakage Suppression

Carrier leakage is a problem that may be present when using variable loads together with a six-port correlator for modulation [16, 23]. The carrier leakage degrades the performance of the transmitter-receiver chain [16, 31, 32]. One approach to limit the effect of carrier leakage is to use balanced modulators [29, 30, 33]. However, balanced modulators require a complex circuit implementation. Here a simple yet efficient method to suppress the carrier leakage is presented.

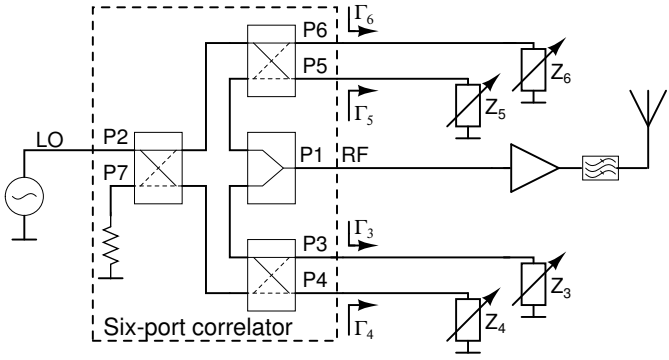

Fig. 3.1: Schematic of six-port modulator/transmitter.

3.1.1 Theory

It was shown in (2.12) in Section 2.2.2 that the presence of a static component of Γ, i.e., $\Gamma_{CM} \neq 0$ generates an unwanted carrier signal at the output port P1 of the six-port modulator. In general the following holds

$$b_1 = -\frac{a_2}{4}\left[(\Gamma_3 + \Gamma_4) + j\left(\Gamma_5 + \Gamma_6\right)\right] \tag{3.1}$$

where Γ_x is the reflection coefficient looking out at port Px of the six-port correlator. The value of Γ_x is dependent on three parameters: a) the load input impedance $Z_{load,x}\left(V_x\right)$, b) the characteristic impedance $Z_{0,x}$ of the transmission line (TL) and c) the length l_x of the TL connecting the output at port Px to the load.

$$\Gamma_{load,x}\left(V_x\right) = \frac{Z_{load,x}\left(V_x\right) - Z_{0,x}}{Z_{load,x}\left(V_x\right) + Z_{0,x}} \tag{3.2}$$

$$\Gamma_x = \Gamma_{load,x} e^{-j2\beta l_x} = \Gamma_{load,x} e^{-j\theta_x} \tag{3.3}$$

where $\theta_x = 2\beta l_x$, $\beta = 2\pi/\lambda$, $\lambda = v_p/f$ and v_p the phase velocity. V_x is a control voltage or baseband signal to change the impedance $Z_{load,x}$ to allow modulation. The same impedance load device (such as a diode or transistor)

is assumed to be used at ports P3 - P6 and, therefore, $\Gamma_{load,x} = \Gamma$ where Γ is the reflection coefficient at the load to TL interface and modeled by (2.10). Hence,

$$\Gamma_x = (\Gamma_{CM} + \Delta\Gamma_x)\, e^{-j\theta_x} = |\Gamma_{CM}+\Delta\Gamma_x| e^{j\angle(\Gamma_{CM}+\Delta\Gamma_x)} e^{-j\theta_x} = |\Gamma| e^{j\angle\Gamma} e^{-j\theta_x} \tag{3.4}$$

where $\Delta\Gamma_x = \delta\Delta v_x$ as previously discussed in Section 2.2.2.

3.1.1.1 Carrier Leakage Suppression Without Modulation

When there is no modulation, i.e., $\Delta v_x = 0$ and $\Delta\Gamma_x = 0$, the requirement on the output signal to have no carrier leakage is that $b_1 = 0$. Using $\Delta\Gamma_x = 0$, (3.1) and (3.4) result in

$$b_1 = -\frac{a_2}{4}|\Gamma_{CM}| e^{j\angle\Gamma_{CM}} \left[\left(e^{-j\theta_3} + e^{-j\theta_4}\right) + j\left(e^{-j\theta_5} + e^{-j\theta_6}\right)\right] \tag{3.5}$$

It is possible to select the values of θ_x in (3.5) to force both the real and imaginary parts to zero, and therefore fulfill $b_1 = 0$. The following two conditions must then be fulfilled:

$$e^{-j\theta_3} = -e^{-j\theta_4} = e^{\pm j\pi} e^{-j\theta_4} \tag{3.6}$$

$$e^{-j\theta_5} = -e^{-j\theta_6} = e^{\pm j\pi} e^{-j\theta_6} \tag{3.7}$$

hence

$$\theta_m = \theta_n \pm \pi \tag{3.8}$$

$$l_m = l_n \pm \frac{\lambda}{4} \tag{3.9}$$

From (3.9) it is clear that the minimum length difference between the TLs at ports (m, n), i.e., (P3, P4) and (P5, P6), must be $\lambda/4$ to avoid carrier leakage. A six-port modulator that fulfills these requirements is shown in Fig. 3.2 and a photo is shown in Fig. 3.3.

It should be noted that the same technique can be used to avoid carrier leakage to the RF port in a corresponding six-port demodulator. Because

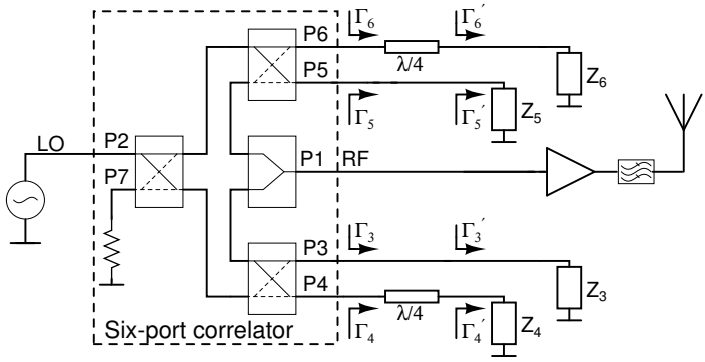

Fig. 3.2: Schematic of six-port transmitter with a carrier leakage suppression technique [20].

any mismatch at the detector diodes in a six-port demodulator will generate a static $\Gamma_{CM} \neq 0$ and thus exactly the same analysis and solution, as discussed here holds for demodulators. Carrier leakage in six-port demodulators is further discussed in Section 4.4.

3.1.1.2 Carrier Leakage Suppression for Modulation

If the requirement for no carrier leakage is satisfied as derived in Section 3.1.1.1, for example by selecting $\theta_3 = \theta_5 = 0$ and $\theta_4 = \theta_6 = \pi$, it follows from (3.4)

$$\Gamma_3 = (\Gamma_{CM} + \Delta\Gamma_3) \tag{3.10}$$

$$\Gamma_4 = -(\Gamma_{CM} + \Delta\Gamma_4) \tag{3.11}$$

$$\Gamma_I = \Gamma_3 + \Gamma_4 = \Delta\Gamma_3 - \Delta\Gamma_4 = \delta\,(\Delta v_3 - \Delta v_4) \tag{3.12}$$

The common and unwanted part Γ_{CM} cancels out and only the modulating part $\Delta\Gamma_x$ remains. The same principle holds for the Q channel, i.e., Γ_Q. To avoid offsetting the IQ constellation, and also to avoid a carrier leakage, the

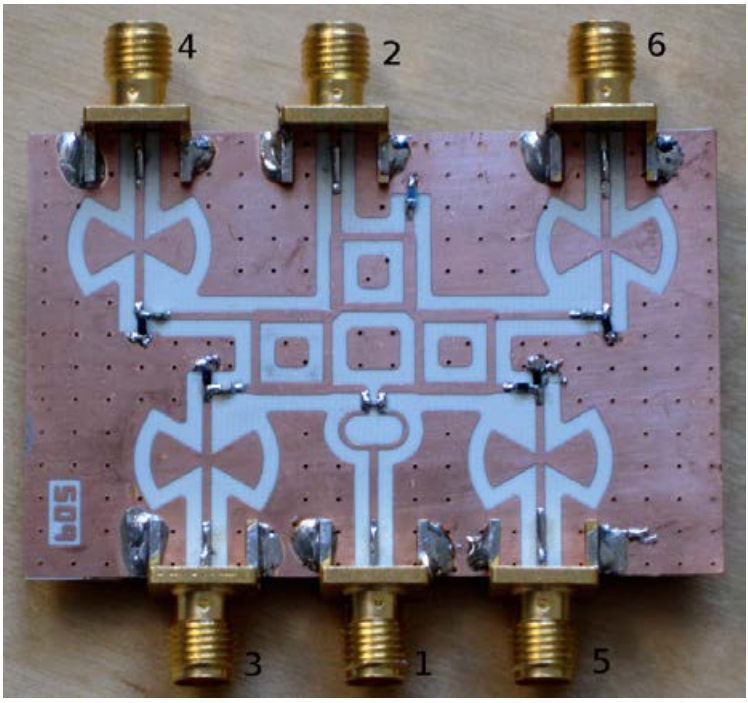

Fig. 3.3: Photo of implemented six-port modulator with a technique for carrier leakage suppression [20].

expected (mean) value of I and Q channel must be zero, i.e.,

$$E\{\Gamma_I\} = E\{\Gamma_Q\} = 0 \tag{3.13}$$

If the voltages on the I-channel are selected according to

$$\Delta v_3 = kX_I \tag{3.14}$$

$$\Delta v_4 = -kX_I = -\Delta v_3 \tag{3.15}$$

where X_I is the modulating symbol for I-channel and k a scaling factor.

Using (3.14) - (3.15) in (3.12)

$$\Gamma_I = 2\delta k X_I \tag{3.16}$$

a similar result holds for the Q-channel

$$\Gamma_Q = 2\delta k X_Q \tag{3.17}$$

and it is assumed that $E\{X_I\} = E\{X_Q\} = 0$ so there is no carrier leakage.

If there is a gain difference ϵ and an offset v_{offset} on Δv_4 compared to Δv_3, i.e.,

$$\Delta v_4 = -kX_I(1+\epsilon) + v_{offset} \tag{3.18}$$

it follows from (3.12) that

$$\Gamma_I = \underbrace{\delta k X_I (1+1+\epsilon)}_{E\{\cdot\}=0} + \underbrace{\delta v_{offset}}_{E\{\cdot\}\neq 0} \tag{3.19}$$

which shows that a gain difference will not generate any carrier leakage. On the other hand, any offset $v_{offset} \neq 0$ will then contribute to the carrier leakage. Another observation is that if $\epsilon = -1$ the value of $\Delta v_4 = 0$, so there is no need to modulate the load connected at port P4, i.e., a single ended baseband control signal can be used. A single ended baseband control signal may simplify the circuit, but will also lower the output power by 6 dB compared to the case when a differential baseband control signal is used (for $\epsilon = 0$). In both cases the common mode voltage V_{CM} (that generates Γ_{CM}) must be the same to suppress the carrier leakage.

3.1.2 Results

A six-port modulator was implemented to verify the carrier leakage suppression technique proposed in this study. The six-port modulator uses an additional $\lambda/4$ transmission line at port P4 and P6 as shown in Fig. 3.2 and Fig. 3.3. The output power spectrum was measured for a QPSK signal at 100

Msymbol/s. As seen in Fig. 3.4 the carrier leakage is efficiently suppressed. Another benefit with the proposed carrier leakage suppression technique, when used with differential baseband control signals, is that it improves the linearity. This is illustrated in Fig. 3.5 for a 16-QAM modulated signal.

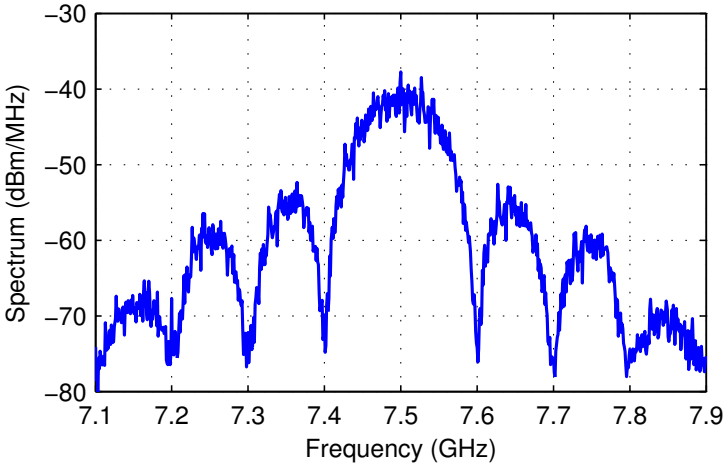

Fig. 3.4: Measured spectrum for a QPSK signal at 100 Msymbol/s. Owing to the use of $\lambda/4$ TL at specific ports the carrier leakage is suppressed [20].

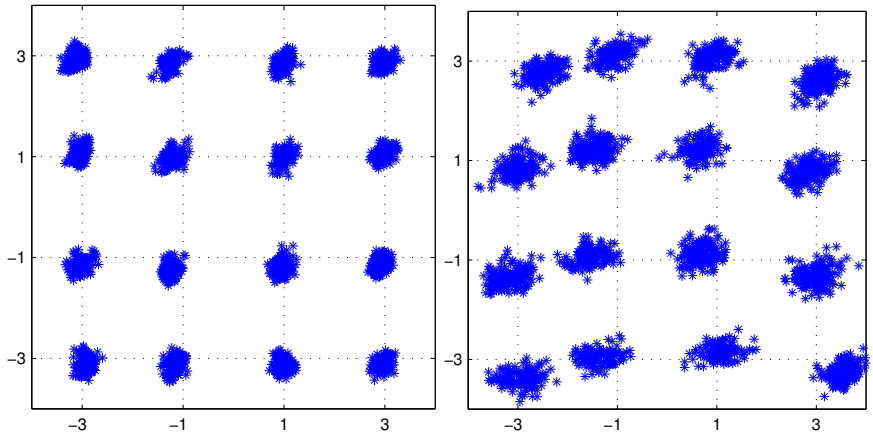

(a) Differential control signal. (b) Non-differential control signal.

Fig. 3.5: Measured constellations for 16-QAM @ 100 Msymbol/s. When differential and non-differential control voltages are used [20].

3.2 Impact of Phase Shifting Network on Carrier Leakage Suppression and EVM

As shown in Section 3.1.1.1, one way to ensure low carrier leakage is to have a 90° phase shift between ports in each port pair (P3, P4) and (P5, P6), respectively. In general the phase shift and amplitude scaling between the ports in a port pair will deviate from their ideal values when the actual frequency deviates from the center (designed) frequency f_0. Operating at a frequency where the amplitude and/or phase shift is not ideal will degrade the carrier leakage suppression and EVM performance. Hence a model to predict the performance as a function of the S-parameters of the phase shifting network is derived. Using the derived model, a wideband phase shifting network is proposed and optimized. A six-port modulator using the wideband phase shifting network is shown in Fig. 3.6.

3.2.1 Theory

The reflection coefficient Γ_x looking out of port Px of the six-port and towards the phase shifting network (the two port network) is given by

$$\Gamma_x = S_{11} + \frac{S_{12}S_{21}\Gamma_{L,x}}{1 - S_{22}\Gamma_{L,x}} \tag{3.20}$$

where $\Gamma_{L,x}$ is the reflection coefficient looking into the impedance load Z_x and modeled according to (2.10), i.e.,

$$\Gamma_{L,x} = \Gamma_{CM} + \Delta\Gamma_x \tag{3.21}$$

The S-parameters for the phase shifting network are assumed to be given by

$$\mathbf{S} = \begin{bmatrix} 0 & Ae^{-j\phi} \\ Ae^{-j\phi} & 0 \end{bmatrix} \tag{3.22}$$

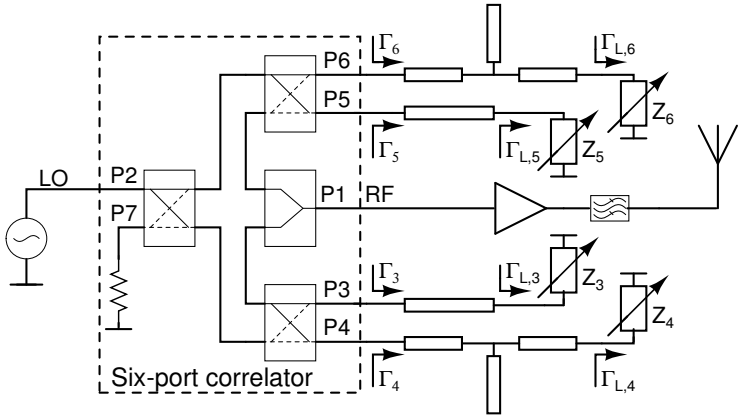

Fig. 3.6: Schematic of the six-port modulator using a broadband phase shifting network to suppress carrier leakage [47].

where $S_{12} = S_{21} = Ae^{-j\phi}$ and A the amplitude scale factor and ϕ the phase shift. Calculating for I-channel $\Gamma_I = \Gamma_3 + \Gamma_4$ and by using $\Delta\Gamma_3 = -\Delta\Gamma_4 = \Delta\Gamma$ it follows from (3.20) - (3.22)

$$\begin{aligned} \Gamma_I &= \Gamma_3 + \Gamma_4 = \Gamma_{L,3} + A^2 e^{-j2\phi}\Gamma_{L,4} \\ &= \underbrace{\Gamma_{CM}\left(1 + A^2 e^{-j2\phi}\right)}_{\text{Carrier leakage}} + \underbrace{\Delta\Gamma\left(1 - A^2 e^{-j2\phi}\right)}_{\text{Modulated RF}} \end{aligned} \tag{3.23}$$

where $\phi = 0$ and $A = 1$ were used for the phase shifting network responsible for Γ_3. As expected from previous analysis, when $A = 1$ and $\phi = 90°$ there is no carrier leakage and $\Gamma_I = 2\Delta\Gamma$. If $A \neq 1$ and/or $\phi \neq 90°$ the Γ_I vector is distorted resulting in both carrier leakage and EVM degradation. Owing to circuit symmetry the same analysis holds for the Q-channel as well.

3.2.1.1 Carrier Leakage Dependence on Amplitude and Phase Mismatch

To find the carrier leakage (3.23) is used with $\Delta\Gamma = 0$. For matched ports, the transmitted output power $P_{TX} = |b_1|^2/2$ is related to the LO power

$P_{LO} = |a_2|^2/2$ by (3.1)

$$P_{TX} = \frac{P_{LO}}{16}\left(|\Gamma_I|^2 + |\Gamma_Q|^2\right) \tag{3.24}$$

The same impedance loads Z_x are assumed to be used on ports P3 - P6, therefore $\Gamma_Q = \Gamma_I$. Using (3.23) in (3.24) it follows that the leakage power ratio $R_{leakage}$ is

$$R_{leakage} = \frac{P_{TX}}{P_{LO}}|_{\Delta\Gamma=0} = \frac{|\Gamma_{CM}|^2}{8}E_f \tag{3.25}$$

where

$$E_f = 1 + A^4 + 2A^2\cos(2\phi) \tag{3.26}$$

is the error function and is dependent on the actual amplitude A and phase ϕ of the phase shifting network. In the ideal case $A = 1$, $\phi = 90°$ and $E_f = 0$, so there is no carrier leakage according to (3.25). Hence by knowing how A and ϕ vary with frequency, i.e., if the S-parameters of the phase shifting network are known, the carrier leakage suppression can be predicted.

3.2.1.2 EVM Dependence on Amplitude and Phase Mismatch

The EVM is given by [48]

$$EVM = \sqrt{\frac{\frac{1}{N}\sum\left(|\Gamma_I - \Gamma_{I,ref}|^2 + |\Gamma_Q - \Gamma_{Q,ref}|^2\right)}{\frac{1}{N}\sum\left(|\Gamma_{I,ref}|^2 + |\Gamma_{Q,ref}|^2\right)}} \tag{3.27}$$

Owing to symmetry both the I and Q channels will be affected in the same way so only the I channel is calculated. The reference (ideal) $\Gamma_{I,ref}$ magnitude square is found by using $A = 1$ and $\phi = 90°$ in (3.23)

$$|\Gamma_{I,ref}|^2 = 4|\Delta\Gamma_I|^2 \tag{3.28}$$

the actual error vector $\Gamma_{I,error}$ is

$$|\Gamma_{I,error}|^2 = |\Gamma_I - \Gamma_{I,ref}|^2 = |\Gamma_{CM} - \Delta\Gamma_I|^2 E_f \tag{3.29}$$

using (3.28) and (3.29) in (3.27) the EVM is then found to be

$$EVM = \sqrt{E_f}\sqrt{\frac{\sum\left(|\Gamma_{CM} - \Delta\Gamma_I|^2 + |\Gamma_{CM} - \Delta\Gamma_Q|^2\right)}{\sum\left(4|\Delta\Gamma_I|^2 + 4|\Delta\Gamma_Q|^2\right)}} \tag{3.30}$$

The EVM is therefore proportional to the square root of the error function E_f. For the special case $\Gamma_{CM} = 0$ there is no carrier leakage according to (3.25) and the EVM is only dependent on E_f as $EVM_{|\Gamma_{CM}=0} = \sqrt{E_f}/2$. The link between EVM and E_f and therefore to the S-parameters of the phase shifting network can be utilized to design a phase shifting network with good performance.

3.2.2 Broadband Phase Shifting Network Using Loaded Transmission Lines

A phase shifting network based on adding a TL of length $\lambda/4$ at specific ports, e.g., at port P4 and P6 as shown in Fig. 3.2, works well for narrow-band applications. However, for more wideband applications, a broadband phase shifting network should be used. Between many possible solutions our approach is based on a loaded transmission line [49]. A six-port modulator using a phase shifting network based on the loaded transmission line is shown in Fig. 3.6. Referring to Fig. 3.7, the references branch is a TL with an electrical length $\phi_r = 270°$. In the other branch a TL of electrical length $2\phi_m = 180°$ is loaded with an open circuit (O.C) stub at the center with length $\phi_s = 180°$. All electrical lengths are defined at the center frequency f_0. Compared to a single TL, the loaded TL helps to keep the phase difference close to 90° over a wider bandwidth. Amplitude and phase variations over frequency depend on the impedances Z_m and Z_s. Hence the phase shifting network can be optimized for carrier leakage suppression and

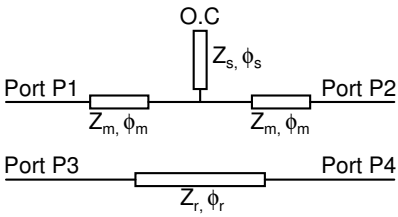

Fig. 3.7: Broadband phase shifter using a loaded transmission line [47].

the minimum EVM degradation, if the optimization goal is to minimize E_f over the frequency range of interest.

3.2.3 Results

Since the use of $\lambda/4$ TL is a narrow-band phase shifting network, the performance will degrade outside of the center frequency. The simulated performance of E_f, and therefore the carrier leakage suppression according to (3.25), for a phase shifting network based on a TL and for the broadband phase shifting network is compared in Fig. 3.8. In the simulation an ideal six-port correlator is used. Hence by implementing the broadband phase shifting network instead of the $\lambda/4$ TL the carrier leakage can be suppressed over a much wider bandwidth. For an EVM of less than 10% requires $E_f \leq -14$ dB. An EVM of less than 10% is achived with the broadband phase shifting network over a relative bandwidth of about 60%, to compare with the relative bandwidth of about 12% for the $\lambda/4$ TL phase shifting network.

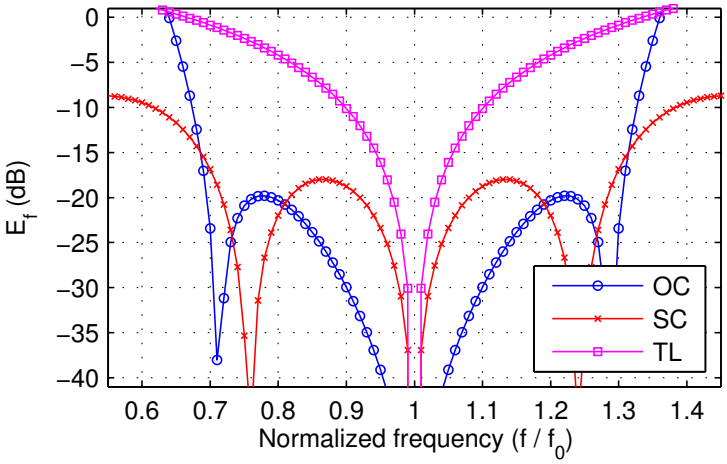

Fig. 3.8: Simulated E_f for a transmission line phase shifting network (TL) and for the optimized broadband phase shifting network terminated with an open circuit (OC) and short circuit (CS) [47].

3.3 Schottky Diode as High-Speed Variable Impedance Load

The technique for carrier leakage suppression can be used with an arbitrary type of impedance load. The optimal type of impedance load to use in a particular situation depends on the actual requirements. Due to its fast speed but low complexity, a Schottky diode is proposed to be used as the variable impedance load instead of a switch or a transistor.

3.3.1 Theory

To model the impedance of the Schottky diode as a function of the applied junction voltage V, the electrical model shown in Fig. 3.9 is used. The series resistor R_s is connected to a voltage-controlled junction resistance $R_j\,(V)$ in parallel with a voltage-controlled junction capacitance $C_j\,(V)$. The following equations are used for modeling:

$$I(V) = I_s\left(e^{\alpha V} - 1\right) \tag{3.31}$$

$$\frac{dI}{dV}|_{V_0} = \alpha I_s e^{\alpha V_0} = \frac{1}{R_j} \tag{3.32}$$

$$C_j(V) = \frac{C_{j0}}{\sqrt{1 - \frac{V}{\Phi}}} \tag{3.33}$$

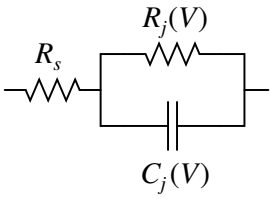

Fig. 3.9: Model used for the Schottky diode [27].

where I_s is the saturation current, $\alpha = n\frac{q}{kT}$, q is the electron charge, k Boltzmann's constant, T the temperature in Kelvin, Φ is the junction potential, and n the ideality factor. Combining (3.31) and (3.32) to express R_j as a function of the current I and I_s:

$$R_j(V) = \frac{1}{\alpha(I(V) + I_s)} \tag{3.34}$$

The junction impedance Z_j, i.e., the parallel combination of R_j and C_j can be expressed as:

$$Z_j = R_{eq} - jX_{eq} \tag{3.35}$$

where

$$R_{eq} = \frac{R_j}{1 + \omega^2 R_j^2 C_j^2} \tag{3.36}$$

$$X_{eq} = \frac{\omega R_j^2 C_j}{1 + \omega^2 R_j^2 C_j^2} \tag{3.37}$$

The parasitic inductance from the package may be absorbed into X_{eq}, and the series resistor R_s in the diode absorbed in R_{eq}.

The junction capacitance $C_j(V)$ and junction resistance $R_j(V)$ are bias dependent according to (3.33) and (3.34). Therefore, the junction impedance Z_j can be controlled by changing the applied voltage V to the diode.

The reflection coefficient Γ, looking into the load from a TL of characteristic impedance Z_0, is given by (3.38). When the diode parameters, LO power and the bias voltage V are known, Γ can be calculated.

$$\Gamma = \frac{Z_j - Z_0}{Z_j + Z_0} = \frac{R_{eq}^2 + X_{eq}^2 - Z_0^2}{(R_{eq} + Z_0)^2 + X_{eq}^2} - j\frac{2X_{eq}Z_0}{(R_{eq} + Z_0)^2 + X_{eq}^2} \tag{3.38}$$

3.3.2 Results

Simulated and measured performance of the Schottky diode based impedance load is presented in the following two sections.

3.3.2.1 Impact of LO Power on Reflection Coefficient

The impedance of the Schottky diode is dependent on the dc current present in the diode, according to (3.31) - (3.37). The dc current is not only dependent on the applied bias voltage, but also on the applied LO power. A part of the applied LO signal is rectified to a dc current and, therefore, contribute to the total dc bias current [50]. To observe the effect of LO power of the reflection coefficient Γ, harmonic balance simulation in Advanced Design System (ADS) from Agilent Technologies Inc. is used. In Fig. 3.10 the reflection coefficient for LO power of -10, -5, 0 and 5 dBm are shown. For low LO power levels, the reflection coefficient is mainly controlled by the applied dc voltage. For high LO power levels, the reflection coefficient Γ is dependent on both the dc bias and the LO power used. The simulation verified the predicted dependence on LO power.

3.3.2.2 Measured Constellations

To verify that the Schottky diode is a suitable solution for high-speed applications, measurements on the prototype modulator have been conducted. In the measurements a 16-QAM modulated signal at 100 and 300 Msymbol/s was used. The corresponding data rates are thus 400 Mbit/s and 1.2 Gbit/s, respectively. The results shown in Fig. 3.11 prove that Schottky diodes can be used to implement variable impedance loads that supports both high order modulation and data rates above 1 Gbit/s in a six-port modulator. Higher symbol rates than 300 Msymbols/s could not be verified due to limitations in the baseband generator that was used.

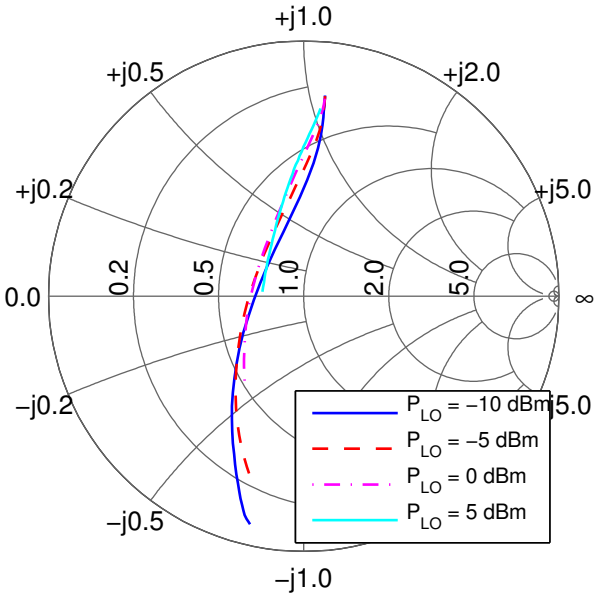

Fig. 3.10: Simulated Γ vs applied voltage and for different values of P_{LO} [27].

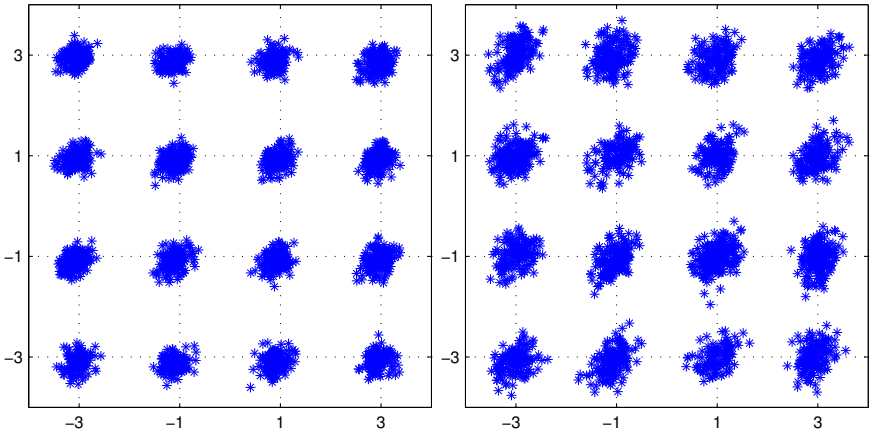

(a) 100 Msymbol/s = 400 Mbit/s. (b) 300 Msymbol/s = 1.2 Gbit/s.

Fig. 3.11: Measured constellations for 16-QAM signal [27].

3.4 Summary

The problem with carrier leakage in a six-port modulator was investigated and a solution presented. Our solution, based on a phase shifting network delivering a 90° phase difference between specific ports, is easy to implement. In its most simple form, a $\lambda/4$ TL may be used.

The performance of the carrier leakage suppression and the modulation performance in terms of EVM were further investigated as a function of the phase shifting network. Both carrier leakage suppression and the EVM performance can be described by the same error function. The error function is directly related to the amplitude and phase behavior of the phase shifting network, i.e., it is related to the S-parameters of the phase shifting network.

For wideband performance, a loaded TL was proposed as one possible solution to implement the phase shifting network. It was designed and optimized with help of the derived error function.

The use of Schottky diodes as high-speed variable impedance loads was proposed and investigated. A six-port modulator using Schottky diodes as variable impedance loads, including the carrier leakage suppression technique was implemented. Measurements verified the carrier leakage suppression technique and showed good modulation performance for a 16-QAM modulated signal with a data rate of 1.2 Gbit/s. The data rate was limited by the available measurement equipment.

4 Six-Port Demodulators in This Study

It was shown in Chapter 2.3 how the six-port correlator can be used together with power detection to recover the baseband signal. In this chapter, the performance of a typical six-port demodulator, see Fig. 4.1, is presented together with improvements of the architecture to support:

- High-speed processing
- Low power consumption
- Low circuit complexity

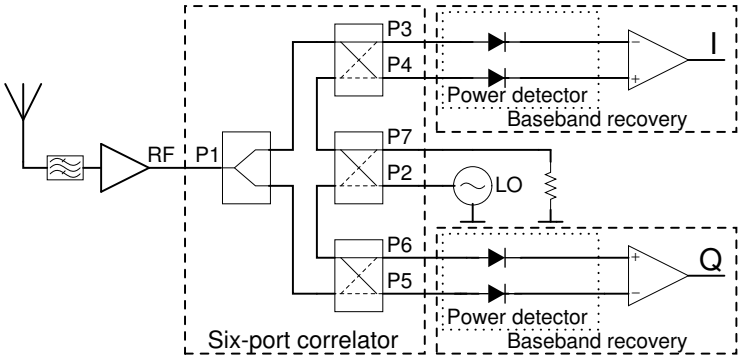

Fig. 4.1: Schematic of a conventional six-port receiver.

4.1 Demodulator for High Data Rate

Six-port demodulators have previously mostly been shown with relatively low date rates, well below 1 Gbit/s [22, 24]. To prove that the six-port is useful for high-speed operation above 1 Gbit/s, a prototype was developed to operate at the upper UWB frequency band with a designed center frequency of 7.5 GHz. The performance of the prototype demodulator is characterized in terms of BER and EVM for different data rates [21].

4.1.1 Theory

It is well known from Shannon's theorem that the channel capacity C is related to the bandwidth B and SNR according to:

$$C = B \log_2 \left(1 + \frac{S}{N}\right) \tag{4.1}$$

The bit rate R_b is related to the symbol rate R_s and modulation order M according to [48]:

$$R_b = R_s \log_2 M \tag{4.2}$$

Using $R_b = 1$ Gbit/s and $M = 16$, i.e., 16-QAM results in $R_s = 250$ Msymbol/s.

According to Shannon's theory and the required symbol rate $R_s = 250$ Msymbol/s, gigabit speed should be possible when operating in the upper UWB 6 - 8.5 GHz due to the wide bandwidth that is available. Hence, the limitations for gigabit speed are not in the six-port correlator itself. For power detection, Schottky diodes are used. Schottky diodes are fast and should not be the limiting factor for gigabit speed. The limitations to achieve high-speed operation are therefore found in the baseband chain: baseband amplifiers and ADCs. These components have been identified as the bottleneck in other studies as well [22, 24]. To build a demodulator that support high-speed, state of the art current mode high-speed operational amplifiers were used to build the baseband amplifier to recover the I and

Q baseband channels, see Fig. 4.2. The measured characteristics of the implemented baseband amplifier, shown in Fig. 4.4, show that the required symbol rate (250 Msymbol/s) to achieve at least 1 Gbit/s is supported.

4.1.2 Measurement Setup

The measurement setup shown in Fig. 4.3 is the basic setup for all demodulator measurements. The I and Q data vectors are generated in a MATLAB program, before they are transfered to the I/Q generator. The analog I and Q channels from the I/Q generator are connected to a vector signal generator to modulate a carrier. The modulated output from the vector signal generator is then fed to the device under test (DUT), i.e., to the RF port of the six-port demodulator. An (ideally) coherent LO signal is connected to the LO port of the six-port demodulator. The baseband I and Q channels at the six-port demodulator are connected to an oscilloscope to sample the waveform. The I and Q waveforms are sampled by a MATLAB program. The received waveform can then be processed and compared with the transmitted waveform to, for example, estimate the EVM and BER performance.

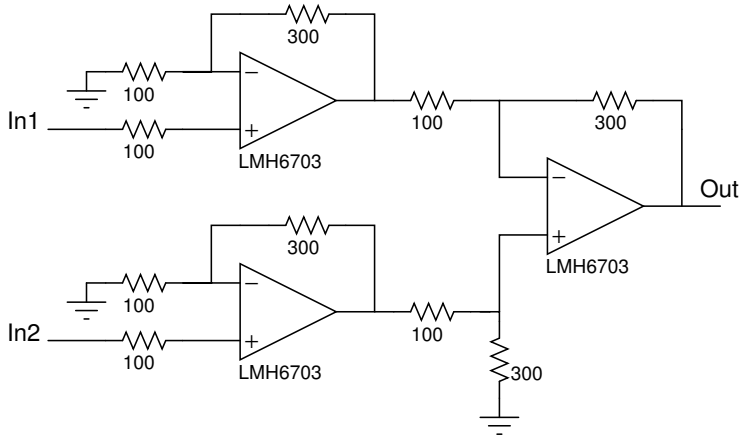

Fig. 4.2: Differential amplifier for baseband recovery [21].

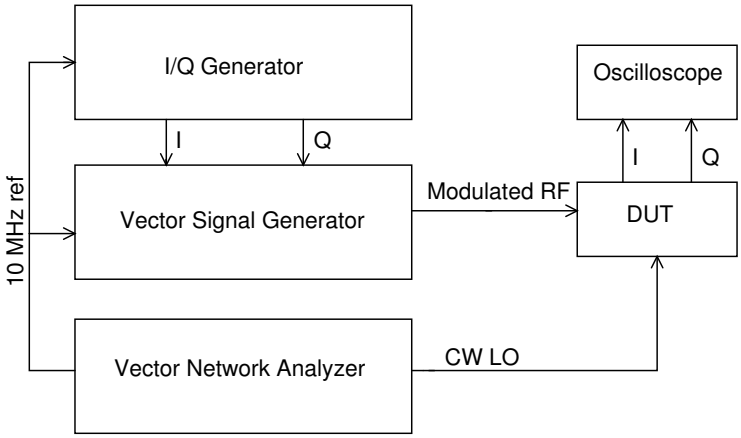

Fig. 4.3: Basic setup for demodulator measurement [21].

4.1.3 Results

The measured forward transmission of the implemented baseband amplifier is shown in Fig. 4.4. Measured constellation for a data rate of $R_b \approx 1.67$ Gbit/s is presented in Fig. 4.5. BER and EVM for different data rates are listed in Table 4.1. Data rates well above 1 Gbit/s have therefore been proved by measurement. Higher data rates may be supported by the six-port demodulator, but the measurement equipment limited us from testing higher data rates.

Table 4.1: Measured BER and EVM for 16-QAM modulated signal [21].

Msymbol/s	Gbit/s	Equalizer	BER	EVM
250	1	yes	$3.63 \cdot 10^{-5}$	10.3
		no	$2.74 \cdot 10^{-4}$	13.5
312.5	1.25	yes	$3.38 \cdot 10^{-5}$	10.7
		no	$9.0 \cdot 10^{-4}$	15.1
416.67	1.67	yes	$4.82 \cdot 10^{-5}$	10.9
		no	$4.04 \cdot 10^{-3}$	18.1

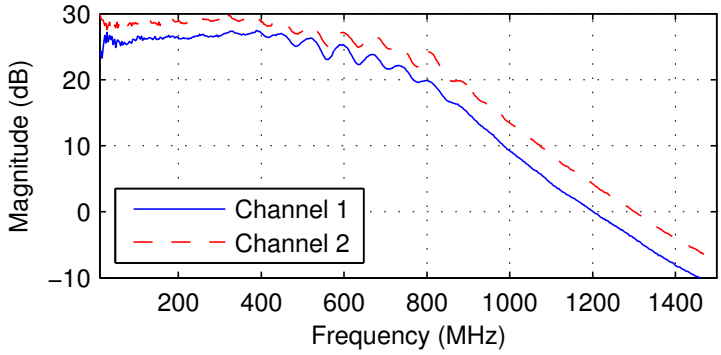

Fig. 4.4: Measured forward transmission (S_{21}) of the baseband amplifier [21].

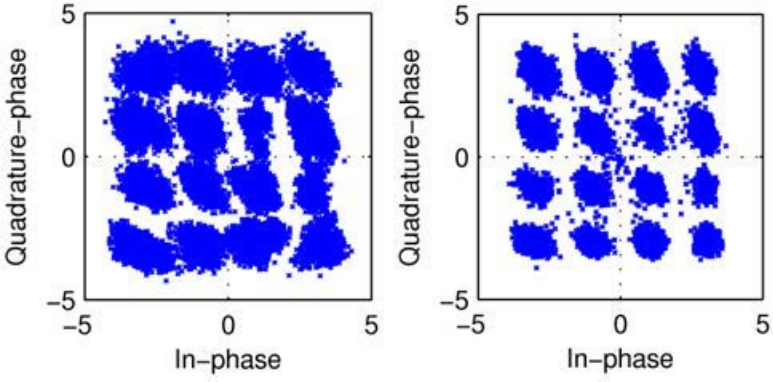

(a) Without equalizer.

(b) With equalizer.

Fig. 4.5: Measured constellation at 1.67 Gbit/s [21].

4.2 Diode Configurations in Six-Port Demodulator

It was shown in Chapter 2.3 that by taking the difference between the diode output current on specific ports, the baseband I and Q channels can be recovered. For instance, to detect the I (Q) channel the difference between V_4 (V_6) and V_3 (V_5) must be calculated according to (2.29) - (2.30). As shown in Fig. 4.1 and Fig. 4.6a, this can be done by using a differential amplifier. However, some drawbacks and limitations can be identified compared to that if an RF transistor is used:

- Speed limitations
- Power consumption
- Complexity and cost

The same drawbacks occur if ADCs are used to sample each of the four output ports directly. Owing to these limitations and drawbacks, an alternative way to recover the baseband I and Q channels that do not require use of differential amplifiers or ADCs are required to support high-speed operation.

The calculation of the difference can also be done by interchanging the diode orientation on one of the diodes on each port pair (P3, P4) and (P5, P6), see Fig. 4.6b. In this way the baseband signal can still be recovered, but there is no need to use a differential amplifier. Avoiding the use of two (I and Q channel) differential amplifiers simplifies the circuit and allows for higher processing speed. If the recovered baseband signal needs to be amplified, a single ended amplifier can be used, such as a RF transistor for high-speed processing.

4.2.1 Theory

Three different approaches to calculate the difference of the signals between port pairs (P3, P4) and (P5, P6) are shown in Fig. 4.6. The configuration

in Fig. 4.6a is commonly used and also useful to model the demodulator. The diode current $i_{d,x}$ at port Px can be approximated by:

$$i_{d,x}\left(v_{d,x}\right) = k_1 v_{d,x} + k_2 v_{d,x}^2 + k_3 v_{d,x}^3 + \cdots \tag{4.3}$$

where $v_{d,x}$ is the applied voltage over the diode junction connected to port Px on the six-port correlator. This voltage is a linear combination of the RF and LO signals applied to the six-port correlator. By using the results

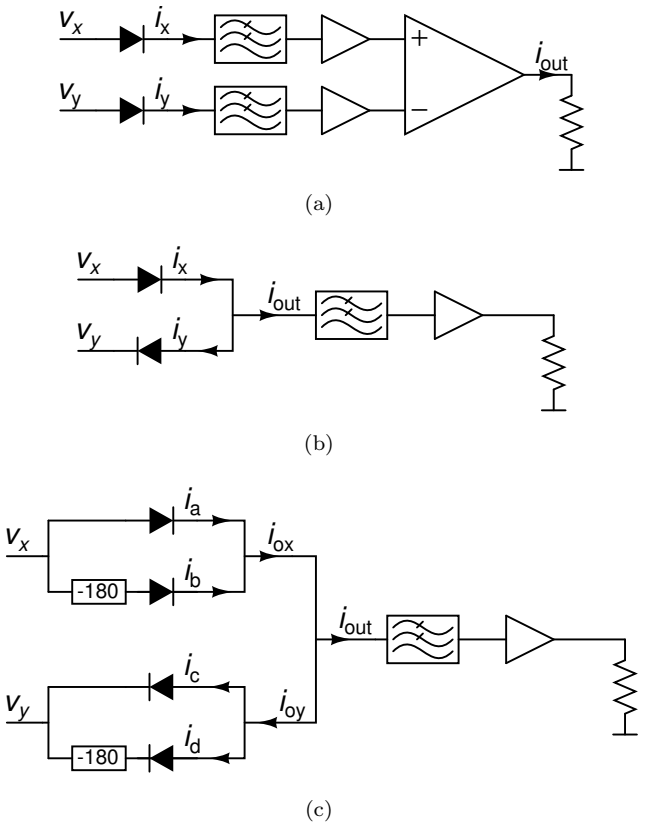

Fig. 4.6: Diode configurations in six-port demodulator [19].

from Section 2.3.2, the voltages and currents related to I-channel is found by using the S-parameters in (2.27) together with (2.14) - (2.17) to get $v_{d,3}$ and $v_{d,4}$:

$$2v_{d,3} = A_{LO}\cos(\omega t) + A_{RF}\left[-X_I\cos(\omega t) + X_Q\sin(\omega t)\right] \tag{4.4}$$

$$2v_{d,4} = -A_{LO}\sin(\omega t) + A_{RF}\left[-X_I\sin(\omega t) - X_Q\cos(\omega t)\right] \tag{4.5}$$

where $\phi = 0$ was assumed. The corresponding currents, assuming $k_n = 0$ for $n \geq 3$, are found from (4.3) to:

$$i_{d,3}(v_{d,3}) = k_1 v_{d,3} + k_2 \left\{ \underbrace{\frac{A_{LO}^2}{8} + \frac{A_{RF}^2}{8}\left(X_I^2 + X_Q^2\right)}_{\text{dc offset}} - \frac{A_{LO}A_{RF}}{4}X_I \right\} + \cdots \tag{4.6}$$

$$i_{d,4}(v_{d,4}) = k_1 v_{d,4} + k_2 \left\{ \underbrace{\frac{A_{LO}^2}{8} + \frac{A_{RF}^2}{8}\left(X_I^2 + X_Q^2\right)}_{\text{dc offset}} + \frac{A_{LO}A_{RF}}{4}X_I \right\} + \cdots \tag{4.7}$$

the "$\cdots$" are terms due to second harmonic frequency components at $2f$, which are assumed to be suppressed together with the fundamental frequency components f by a low-pass filter. The bracket part $\{\cdot\}$ in (4.6) - (4.7) describes signals at dc, it includes the wanted baseband signal together with unwanted dc offset.

4.2.2 Baseband Recovery with Differential Amplifier

If a differential amplifier, as shown in Fig. 4.6a, is used to take the difference:

$$i_{out} = G\left(i_{d,4}(v_{d,4}) - i_{d,3}(v_{d,3})\right) \tag{4.8}$$

the output signal after low-pass filtering, i.e., the baseband signal is:

$$i_{out,BB} = Gk_2 \frac{A_{LO} A_{RF}}{2} X_I \tag{4.9}$$

where G is the gain of the differential amplifier. The three main reasons to calculate the difference, found by inspecting (4.6) - (4.7), are to:

- Double the amplitude of the wanted baseband signal
- Suppress the static dc part from the LO source
- Suppress the dynamic dc offset from rectification of I and Q data

4.2.3 Baseband Recovery without Differential Amplifier

To avoid the use of a differential amplifier, the anode-cathode side of one of the diodes (in this case the diode related to $i_{d,3}$) may be interchanged as shown in Fig. 4.6b and the output current is:

$$i_{out} = i_{d,4}\left(v_{d,4}\right) - i_{d,3}\left(-v_{d,3}\right) \tag{4.10}$$

However, $k_2\left(v_d\right)^2 = k_2\left(-v_d\right)^2$ so after low-pass filtering the baseband signal is:

$$i_{out,BB} = k_2 \frac{A_{LO} A_{RF}}{2} X_I \tag{4.11}$$

therefore, the only difference between (4.9) and (4.11) is the gain factor G. This gain can easily be compensated for by using a single ended amplifier after the low-pass filter, see Fig. 4.6b. To relax the requirement on the low-pass filter, the diode configuration shown in Fig. 4.6b can be modified to the one shown in Fig. 4.6c. The additional benefit is that odd-order harmonics are suppressed due to the relative phase difference of 180° at the fundamental frequency between the two parallel diode pairs.

4.2.4 Results

The demodulation performance was measured for a 16-QAM signal at 100 Msymbol/s, i.e., a data rate of 400 Mbit/s. The RF and LO inputs are directly applied to the six-port correlator and the recovered I and Q baseband signals are measured and compared with the transmitted I and Q signals for EVM calculation. No impedance matching was used for the diodes. Hence, performance may likely be improved by using impedance matching at the cost of a more complex circuit.

4.2.4.1 Constellation

The measured constellations at the sensitivity limit, i.e., for a BER $\leq 10^{-3}$ is shown in Fig. 4.7 where the diode configuration shown in Fig. 4.6b and Fig. 4.6c is used. Good performance and high-speed operation are therefore possible without the use of differential amplifiers. The measured sensitivity levels are -33 and -44 dBm at a LO power of 6 dBm for the diode configura-

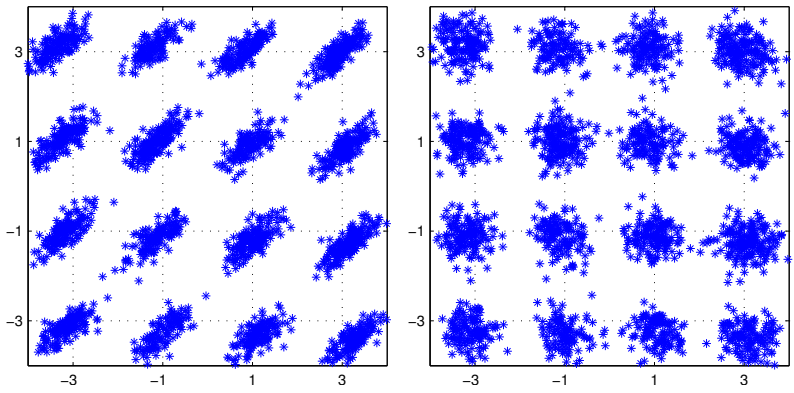

(a) Diode configuration without harmonic suppression.

(b) Diode configuration with harmonic suppression.

Fig. 4.7: Measured constellations for 16-QAM modulation at 100 Msymbol/s [28].

tion without (see Fig. 4.6b) and with (see Fig. 4.6c) harmonic suppression, respectively.

4.2.4.2 EVM

The EVM for different LO power levels $P_{LO} \in \{3, 6, 9\}$ dBm, and when the RF power is sweped from $P_{RF} = -45$ dBm to $P_{RF} = 0$ dBm is shown in Fig. 4.8. The EVM in Fig. 4.8b shows a more flat and lower EVM vs RF power compared to the EVM in Fig. 4.8a. In this case, better EVM performance over a larger RF power range can be achieved when the diode configuration with odd-order harmonic suppression is used.

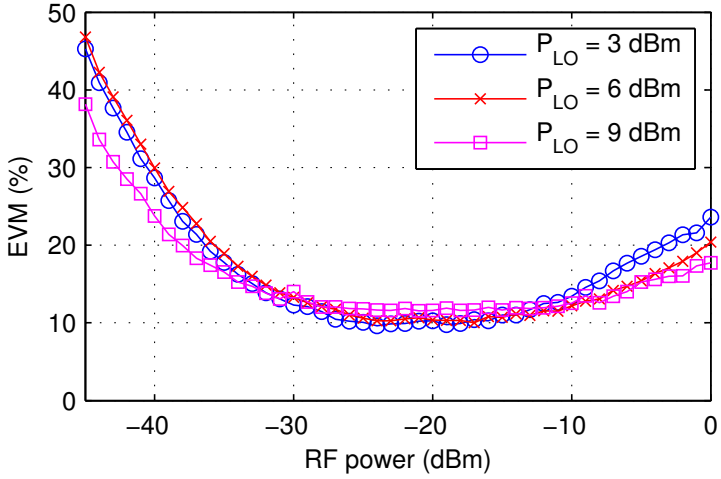

(a) Diode configuration without harmonic suppression.

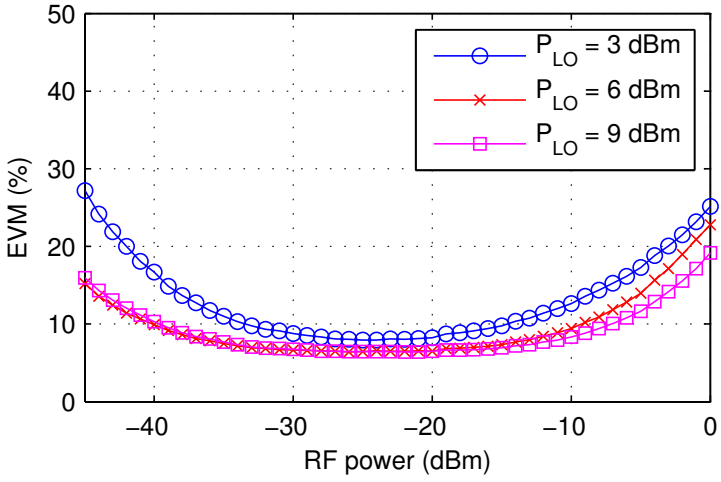

(b) Diode configuration with harmonic suppression.

Fig. 4.8: Measured EVM for 16-QAM modulation at 100 Msymbol/s [28].

4.3 Baseband Complexity Comparison of Six-, Five-, and Four-Port Demodulators

With the new diode configurations that allows high-speed processing, the circuit complexity was reduced which also implies that the power consumption can be decreased. Other multi-port structures, like the five-port and four-port, have also been proposed to simplify the complexity in recovering the baseband signal. In a five-port receiver only three ports are used for baseband recovery and in a four-port receiver two ports are used to recover the baseband data. It can be shown mathematically that three output ports are required to demodulate, i.e., to recover the baseband data. Hence, a six-port has one "extra" port that is not strictly required, but simplifies the baseband receovery circuit. The four-port receiver only works with some additional constraints on the RF and LO signals.

4.3.1 Analysis of Baseband Complexity

In a six-port receiver shown in Fig. 4.1 there are four outputs (P3 - P6) and hence four equations are available. There is one more equation than unknown variables. Therefore, one equation can be removed, i.e., one of the output port can be removed. This results in a five-port [37, 51, 52]. The three remaining outputs allow to calculate X_I, X_Q and $R = X_I^2 + X_Q^2$. One possible configuration of a five-port receiver is shown in Fig. 4.9 [51]. Using the same approach as in Section 2.3.2, the corresponding equation in matrix form is then

$$\begin{bmatrix} L_3 & N_3\cos\angle S_3 & N_3\sin\angle S_3 \\ L_4 & N_4\cos\angle S_4 & N_4\sin\angle S_4 \\ L_5 & N_5\cos\angle S_5 & N_5\sin\angle S_5 \end{bmatrix} \begin{bmatrix} R \\ X_I \\ X_Q \end{bmatrix} = \begin{bmatrix} V_3' \\ V_4' \\ V_5' \end{bmatrix} \tag{4.12}$$

where $V_x' = V_x - M_x$. The $\mathbf{D}$ matrix is found by inspection of the S-parameters for the five-port configuration shown in Fig. 4.9:

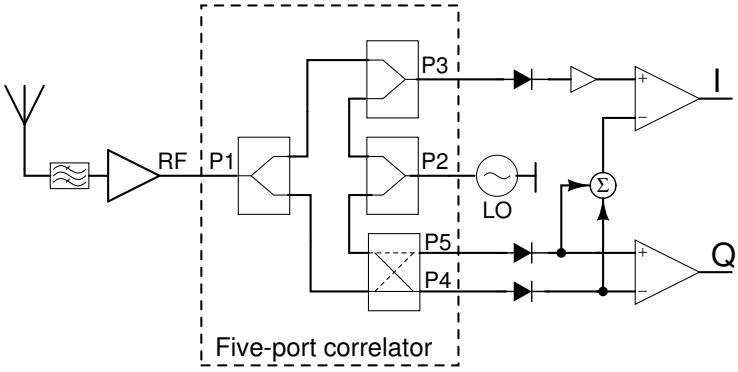

Fig. 4.9: Schematic of five-port receiver [53].

$$\mathbf{D_5} = \frac{1}{8}\begin{bmatrix} A_{RF}^2 & 2A_{LO}A_{RF} & 0 \\ A_{RF}^2 & 0 & -2A_{LO}A_{RF} \\ A_{RF}^2 & 0 & 2A_{LO}A_{RF} \end{bmatrix} \tag{4.13}$$

from which the I and Q channels for $\mathbf{D_5}$ are calculated to be

$$I = \frac{2}{A_{LO}A_{RF}}\left(2V_3 - V_5 - V_4\right) \tag{4.14}$$

$$Q = \frac{2}{A_{LO}A_{RF}}\left(V_5 - V_4\right) \tag{4.15}$$

This shows that it is possible to derive the Q channel with the difference between two outputs, but the I channel must be calculated by considering three outputs, as shown in (4.14). Because of this, at least one differential amplifier is required on each of the I and Q channels to recover I and Q data. It is not possible to simply change the direction on specific diodes to avoid the use of differential amplifiers, as in the case for the six-port receiver. The five-port can therefore not utilize the same advantage of the diode configurations and hence the six-port allows for a simpler baseband recovery circuit.

4.3.2 Performance Comparison

The implementation complexity to implement the six-, five-, and four-port demodulators is listed in Table 4.2. For performance comparison, the EVM for six-, five-, and four-port demodulators is compared versus frequency, see Fig. 4.10. This shows that the six-port demodulator, in contrast to the five- and four-port demodulators, has a) the best performance and b) the lowest complexity when used together with the new diode configurations. The five-port cannot take advantage of the diode configurations to avoid differential amplifiers and hence its speed may be limited.

Table 4.2: Implementation complexity of six-, five- and four-port demodulators.

	Six-Port	Five-Port	Four-Port
Power detectors	4	3	2
ADCs, if no analog processing	4	3	2
ADCs, after analog processing	2	2	2
Support simplified diode configurations	yes	no	N/A

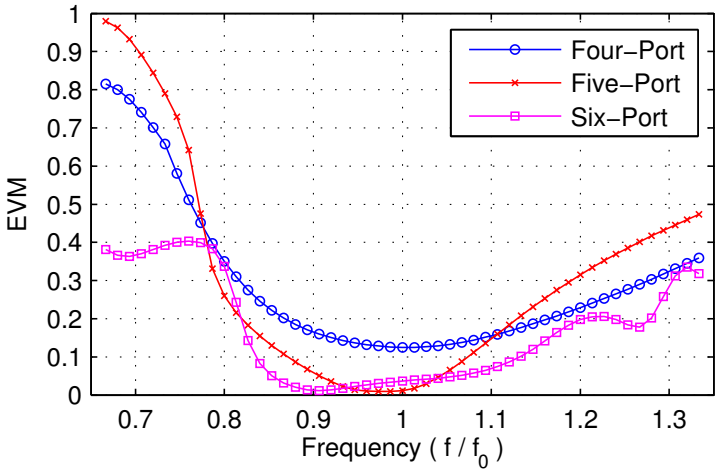

Fig. 4.10: EVM comparison for six-, five-, and four-port demodulator [53].

4.4 Carrier Leakage Suppression

The carrier leakage, or LO leakage, problem in a modulator was discussed in Section 3.1. Carrier leakage in a six-port demodulator is also a problem.

It is well-known that in direct conversion receivers (like a six-port demodulator), the LO leakage to the RF port may results in dc offset, noise and second-order distortion that may result in decreased receiver sensitivity and reduced dynamic range [34–36]. A part of the LO signal that leaks to the RF input port may also reach the antenna, resulting in unwanted in-band emission of the LO signal that may disturb other receivers [34]. The in-band emission may also be reflected in the environment and received by the six-port demodulator itself. The presence of carrier leakage in a six-port demodulator therefore severely degrades the system performance.

4.4.1 Theory

With respect to the different reflection coefficients present on specific port of the six-port correlator, the theory derived in Section 3.1 for carrier leakage suppression in a six-port modulator then holds for a six-port demodulator as well. The main difference is that in a modulator, the reflection coefficients change with time to allow for modulation, hence $\Delta\Gamma_x \neq 0$ in a modulator. In a six-port demodulator, the reflections coefficients are static, hence $\Delta\Gamma_x = 0$ in a demodulator. In both cases the static, or common mode, reflection coefficient Γ_{CM} may be non-zero, resulting in carrier leakage. The total reflection coefficient at port Px is given by:

$$\Gamma_x = \Gamma_{CM} + \Delta\Gamma_x \tag{4.16}$$

Two different approaches to avoid LO leakage to the RF port in a six-port demodulator can thus be identified. The first method is to use the carrier leakage suppression technique, i.e., to implement a phase shifting network to have a phase difference of 90° between specific ports in the six-port correlator.

The other method is to use impedance matching of the diodes so $\Gamma_{CM} = 0$ can be achieved. The power delivered to the load (diode) at port Px is

$$P_{load,x} = |b_x|^2 \left(1 - |\Gamma_x|^2\right) \tag{4.17}$$

To increase the power delivered to the load, $\Gamma_x = \Gamma_{CM}$ ($\Delta\Gamma_x = 0$ in a demodulator) must be minimized.

By using impedance matching of the diodes, the power delivered to the detector diodes is increased and at the same time the carrier leakage is suppressed. The impedance of a diode is dependent on both frequency and power, therefore good matching is only possible at a limited power and limited frequency range. In contrast to using diode matching, the carrier leakage suppression technique is only frequency dependent. For best performance both techniques can be used together.

4.4.2 Results

The measured transmission from LO to RF port (S_{12}) in a demodulator is shown in Fig. 4.11 for different LO power levels and both with and without the carrier leakage suppression technique. The carrier leakage suppression was implemented by using $\lambda/4$ transmission lines and is therefore a narrowband solution. Low LO leakage to the RF port is observed close to the design frequency.

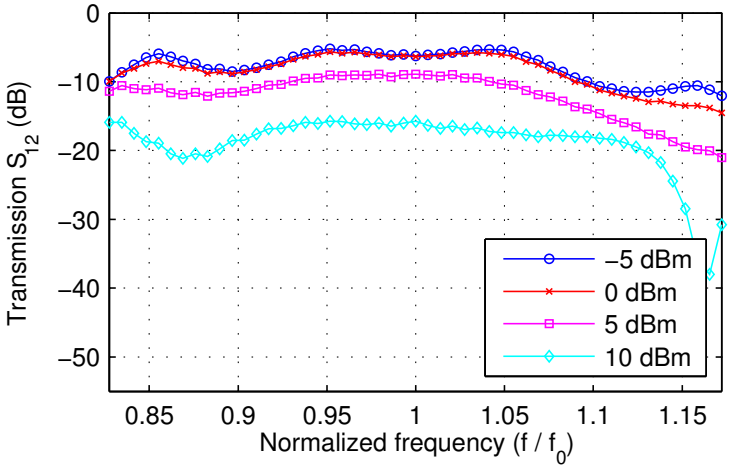

(a) Measured transmission without carrier leakage suppression technique.

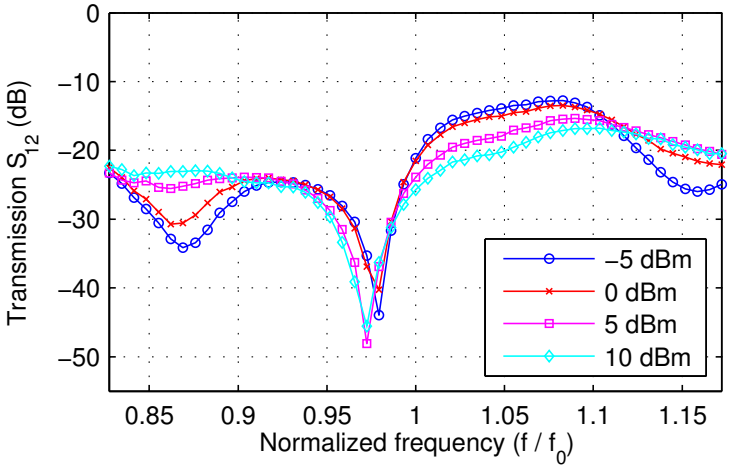

(b) Measured transmission with carrier leakage suppression technique.

Fig. 4.11: Measured transmission (S_{12}) with and without the carrier leakage suppression technique implemented with $\lambda/4$ transmission lines [54].

4.5 Summary

Both the performance and implementation complexity of a six-port demodulator have been investigated. To verify that high data rates above 1 Gbit/s is possible, a six-port demodulator was designed to operate at a center frequency of 7.5 GHz. Measurements on a 16-QAM modulated signal have verified that a data rate of 1.67 Gbit/s was possible with an acceptable BER/EVM performance, see Table 4.1. Higher data rates could not be tested due to limitations in the available measurement equipment.

Differential amplifiers are commonly used in six-port demodulators to recover the baseband I and Q signals. However, for high data rate applications, the differential amplifiers need to operate at high-speed. High-speed differential amplifiers may be both difficult to implement and also, due to high-speed operation, the amplifiers tend to consume much power. To avoid these drawbacks, new diode configurations were proposed. The new diode configurations allow to recover the baseband I and Q data, without the use of differential amplifiers. The new diode configurations allow high data rates but still a low power consumption is maintained.

Other multiport structures, like the five-port and four-port, can also be used for demodulation. The performance and complexity of a six-port, five-port and four-port were compared. The six-port, together with the proposed diode configurations, allows for lower baseband complexity and better EVM vs frequency performance in comparison with the five-port and four-port receivers.

Carrier leakage in a six-port demodulator degrades the receiver performance and two approaches, that can be used independently or together, to suppress the carrier leakage were discussed: diode matching and the use of a phase shifting network. Diode matching is both frequency and power dependent, but allows to increase the power delivered to the diodes. The use of a phase shifting network is on the other hand only frequency dependent.

5 Contributions and Future Work

This part includes the author's main contributions and ideas for future work related to the six-port radio technique.

5.1 Contributions

The author's main contributions and achievements with respect to the six-port modulator and demodulator can be found in the following papers:

Paper 1: Direct Carrier Six-Port Modulator Using a Technique to Suppress Carrier Leakage

Authors: J. Östh, Owais, M. Karlsson, A. Serban, S. Gong, and P. Karlsson

Published in IEEE Transactions on Microwave Theory and Techniques, vol. 59, no. 3, pp. 741–747, 2011.

Abstract: This paper presents a direct carrier six-port modulator. To allow arbitrary load impedances to be used and for suppression of carrier leakage, a new circuit architecture with a technique to suppress carrier leakage is proposed and implemented. A theoretical model of the proposed modulator is derived. A prototype modulator utilizing diodes for impedance generation is designed and fabricated for a center frequency of 7.5 GHz for verification of the proposed technique. Measurements show good modulation properties when a 16 quadrature amplitude modulation signal at 100 Msymbol/s is generated, as well as good carrier leakage suppression.

Author's contribution: The author proposed the concept, performed analysis, simulations, measurements and wrote the article.

Paper 2: Carrier Leakage Suppression and EVM Dependence on Phase Shifting Network in Six-Port Modulator

Authors: J. Östh, M. Karlsson, A. Serban, and S. Gong

Accepted for presentation at Proc. Int. Conf. Microwave and Millimeter Wave Technology ICMMT 2012.

Abstract: In six-port modulators a phase shifting network on specific ports can be used to suppress the carrier leakage that may be present if this network is not present. A model is derived to predict the carrier leakage suppression and error vector magnitude (EVM) as a function of the phase shifting network S-parameters. Both carrier leakage suppression and EVM can be expressed by the same error function. The error function can be used to find the allowed amplitude and phase mismatch in the phase shifting network, or to optimize the performance of a phase shifting network over a given frequency range. A broadband phase shifting network, based on a loaded transmission line, is designed and optimized to operate at a relative bandwidth of 60% for an EVM $< 10\%$. This should be compared to a phase shifting network based on a single transmission line with a corresponding bandwidth of only 12%. The broadband phase shifting network is useful for six-port modulators with carrier leakage suppression, targeting UWB applications.

Author's contribution: The author proposed the concept, performed analysis, simulations and wrote the article.

Paper 3: Schottky Diode as High-Speed Variable Impedance Load in Six-Port Modulators

Authors: J. Östh, Owais, M. Karlsson, A. Serban, and S. Gong

Published in Proc. IEEE Int Ultra-Wideband (ICUWB) Conf, 2011, pp. 68–71.

Abstract: The use of Schottky diodes as high-speed variable impedance loads in six-port modulators are proposed and analyzed in this paper. The impedance dependency of diode parameters and local oscillator power are investigated by theoretical analysis and simulations. A prototype for a direct

carrier six-port modulator using Schottky diodes for impedance generation is designed and fabricated for a center frequency of 7.5 GHz. Measurements show good modulation properties when a 16 quadrature amplitude modulation signal at 300 Msymbol/s is generated, i.e., at a data rate of 1.2 Gbit/s, validating the use of Schottky diodes as high-speed variable impedance loads in six-port modulators.

Author's contribution: The author proposed the concept, performed analysis, simulations, measurements and wrote the article.

Paper 4: Six-Port Gigabit Demodulator

Authors: J. Östh, A. Serban, Owais, M. Karlsson, S. Gong, J. Haartsen, and P. Karlsson

Published in IEEE Transactions on Microwave Theory and Techniques, vol. 59, no. 1, pp. 125–131, 2011.

Abstract: This paper presents measurement results for a six-port-based demodulator designed for a center frequency of 7.5 GHz and with a bandwidth of 1 GHz for operation in the ultra-wideband band. The demodulator includes the six-port correlator, diodes, and amplifiers needed to recover the baseband data. Measurement results show that the prototype supports data rates at 1.7 Gbit/s with bit-error rate $5 \cdot 10^{-5}$ if a two-tap linear equalizer is used and bit-error rate $4 \cdot 10^{-3}$ if only threshold detection is used. The measured performance of the used six-port correlator including the amplifiers is presented and their influence on the overall system performance is discussed. Limitations in the present system and possible improvements are also considered.

Author's contribution: The author proposed the concept, performed analysis, simulations, measurements and wrote the article.

Paper 5: Diode Configurations in Six-Sort receivers with Simplified Interface to Amplifier and Filter

Authors: J. Östh, A. Serban, Owais , M. Karlsson, S. Gong, J. Haartsen, and P. Karlsson

Published in Proc. IEEE Int Ultra-Wideband (ICUWB) Conf, vol. 1, 2010, pp. 1–4.

Abstract: This paper presents two new diode configurations for use with six-port based demodulators. The first proposed diode configuration allows a simplified diode to filter/amplifier interface. The second configuration allows for full-wave rectification and suppression of odd-order harmonics. A demodulator prototype utilizing the new diode concept is designed for a center frequency of 7.5 GHz and with a bandwidth of 1 GHz for verification. The demodulator includes the six-port correlator, diodes and amplifiers needed to recover the baseband data.

Author's contribution: The author proposed the concept, performed analysis, simulations, measurements and wrote the article.

Paper 6: Performance Evaluation of Six-Port Receivers with Simplified Interface to Amplifier and Filter

Authors: J. Östh, Owais, M. Karlsson, A. Serban, and S. Gong

Published in Proc. IEEE Int Ultra-Wideband (ICUWB) Conf, 2011, pp. 190–194.

Abstract: The performance of two different six-port demodulator prototypes for the UWB band 6 to 8.5 GHz are presented. Both configurations allow for a simplified interface to amplifier and filter. In addition, one of the configurations also have odd-order harmonic suppression. Measurements show good modulation properties when a 16 quadrature amplitude modulation signal at 100 Msymbols/s is demodulated for both prototypes. The performance of the two prototypes are compared in terms of error vector magnitude, bit error rate, sensitivity and dynamic range.

Author's contribution: The author proposed the concept, performed analysis, simulations, measurements and wrote the article.

Paper 7: Data and Carrier Interleaving in Six-Port Receivers for Increased Data Rate

Authors: J. Östh, Owais, M. Karlsson, A. Serban, and S. Gong

Published in Proc. IEEE Int Ultra-Wideband (ICUWB) Conf, vol. 1, 2010, pp. 1–4.

Abstract: This paper proposes how antenna polarization can be utilized to increase the maximum data rate in a multiple six-port receiver system. By utilizing data and carrier interleaving, the total information bandwidth increases and therefore the maximum data rate. Prototype antennas were manufactured and the measured results were later used in a simulation model with three channels for verification of the concept.

Author's contribution: The author proposed the concept, performed analysis, simulations, measurements and wrote the article.

Paper 8: Baseband Complexity Comparison of Six-, Five- and Four-Port Receivers

Authors: J. Östh, M. Karlsson, Owais, A. Serban, and S. Gong

Published in Microwave and Optical Technology Letters, vol. 54, no. 6, pp. 1502–1506, 2012.

Abstract: The use of six-port correlators to implement six-port receivers have been intensively studied. The six-port receiver can also be modified to a five-port or a four-port receiver. However, the six-port, five-port or four-port receiver solution requires different baseband processing to recover the baseband In-phase (I) and Quadrature-phase (Q) data. A unified mathematical model for the six-, five- and four-port receivers is presented in this paper. Possible solutions to recover the baseband data are discussed and compared. The investigation shows that the six-port receiver has advantages over the five- and four-port receivers in term of complexity when analog baseband processing is used. Simulations are conducted to verify the model and to estimate the error vector magnitude versus frequency, the simulation also shows that the six-port receiver operates over a wider bandwidth than the five- or four-port receiver.

Author's contribution: The author proposed the concept, performed analysis, simulations and wrote the article.

Paper 9: LO Leakage in Six-Port Modulators and Demodulators and its Suppression Techniques

Authors: J. Östh, A. Serban, M. Karlsson, and S. Gong

Accepted for presentation at Proc. IEEE MTT-S Int. Microwave Symp. (IMS 2012).

Abstract: In a six-port demodulator utilizing diodes for power detection, impedance mismatch at the interface between the six-port correlator and diodes generates unwanted local oscillator (LO) leakage to the radio frequency (RF) port. A six-port modulator that uses variable reflection coefficients at specific ports to generate a modulated RF may also suffer from LO leakage if there is a static part in the reflection coefficient. It is known that LO leakage to the RF port not only generates unwanted emission of the LO signal, but also degrades the receiver system performance due to a dynamic dc offset and second-order non-linearity at the detected baseband signal. How this LO leakage appears to the RF port in six-port demodulators and modulators are analyzed. Two different approaches to suppress the LO leakage is then discussed: a) diode impedance matching and b) introduction of a $\lambda/4$ line on specific ports. The performance when $\lambda/4$ lines are used on specific ports is verified by measurement for both a demodulator and a modulator. The measurement shows high suppression of the LO leakage.

Author's contribution: The author proposed the concept, performed analysis, simulations, measurements and wrote the article.

5.2 Future Work

It is the author's opinion that the six-port radio technique for high-speed data communications is very interesting and hence, there are many possibilities for further work. For example:

- To improve performance of the six-port modulator, it may be interesting to investigate the possibility to design a passive network that can do pulse shaping, such as Root-raised-cosine filtering.

- Techniques for carrier recovery suitable for use with six-port radio.
- Design and implement an analog decoder circuit for 16-QAM or higher order demodulation, including crosstalk compensation.

Bibliography

[1] S. B. Cohn and N. P. Weinhouse, "An automatic microwave phase measurement system," *Microwave J.*, vol. 7, pp. 49–56, 1964.

[2] G. F. Engen and C. A. Hoer, "Application of an arbitrary 6-port junction to power-measurement problems," *IEEE Transactions on Instrumentation and Measurement*, vol. 21, no. 4, pp. 470–474, 1972.

[3] G. F. Engen, "The six-port reflectometer: An alternative network analyzer," *IEEE Transactions on Microwave Theory and Techniques*, vol. 25, no. 12, pp. 1075–1080, 1977.

[4] J. Li, R. G. Bosisio, and K. Wu, "A six-port direct digital millimeter wave receiver," in *Proc. IEEE MTT-S Int. Microwave Symp. Digest*, 1994, pp. 1659–1662.

[5] Y. Zhao, C. Viereck, J. F. Frigon, R. G. Bosisio, and K. Wu, "Direct quadrature phase shift keying modulator using six-port technology," *Electronics Letters*, vol. 41, no. 21, pp. 1180–1181, 2005.

[6] V. Bilik, V. Raffaj, and J. Bezek, "A new extremely wideband lumped six-port reflectometer," in *Proc. 20th European Microwave Conf*, vol. 2, 1990, pp. 1473–1478.

[7] T. Eireiner, T. Schnurr, and T. Muller, "Integration of a six-port receiver for mm-wave communication," in *Proc. IEEE Mediterranean Electrotechnical Conf. MELECON 2006*, 2006, pp. 371–376.

[8] P. Hakansson and S. Gong, "Ultra-wideband six-port transmitter and receiver pair 3.1–4.8 ghz," in *Proc. Asia-Pacific Microwave Conf. APMC 2008*, vol. 2, no. 1, 2008, pp. 1–4.

[9] D. Hammou, N. Khaddaj Mallat, E. Moldovan, S. Affes, K. Wu, and S. O. Tatu, "V-band six-port down-conversion techniques," in *Proc. Int. Symp. Signals, Systems and Electronics ISSSE '07*, 2007, pp. 379–382.

[10] T. Hentschel, "The six-port as a communications receiver," *IEEE Transactions on Microwave Theory and Techniques*, vol. 53, no. 3, pp. 1039–1047, 2005.

[11] J. Hyyrylainen, L. Bogod, S. Kangasmaa, H.-O. Scheck, and T. Ylamurto, "Six-port direct conversion receiver," in *Proc. 27th European Microwave Conf*, vol. 1, 1997, pp. 341–346.

[12] A. Koelpin, G. Vinci, B. Laemmle, D. Kissinger, and R. Weigel, "The six-port in modern society," *IEEE Microwave Magazine*, vol. 11, no. 7, pp. 35–43, 2010.

[13] Z. Lan and W. Bing, "Study on six-port demodulator with anti-parallel diode pair detection," in *Proc. Int. Forum Information Technology and Applications IFITA '09*, vol. 2, 2009, pp. 294–298.

[14] J. Li, R. G. Bosisio, and K. Wu, "A six-port direct digital millimeter wave receiver," in *Proc. IEEE National Telesystems Conf.*, 1994, pp. 79–82.

[15] H.-S. Lim, W.-K. Kim, J.-W. Yu, H.-C. Park, W.-J. Byun, and M.-S. song, "Compact six-port transceiver for time-division duplex systems," *IEEE Microwave and Wireless Components Letters*, vol. 17, no. 5, pp. 394–396, 2007.

[16] B. Luo and M. Y.-W. Chia, "Performance analysis of serial and parallel six-port modulators," *IEEE Transactions on Microwave Theory and Techniques*, vol. 56, no. 9, pp. 2062–2068, 2008.

[17] B. Luo and M. Y. W. Chia, "Direct 16 qam six-port modulator," *Electronics Letters*, vol. 44, no. 15, pp. 910–911, 2008.

[18] N. K. Mallat and S. O. Tatu, "Six-port receiver in millimeter-wave systems," in *Proc. ISIC Systems, Man and Cybernetics IEEE Int. Conf*, 2007, pp. 2693–2697.

[19] J. Osth, A. Serban, O. , M. Karlsson, S. Gong, J. Haartsen, and P. Karlsson, "Diode configurations in six-port receivers with simplified interface to amplifier and filter," in *Proc. IEEE Int Ultra-Wideband (ICUWB) Conf*, vol. 1, 2010, pp. 1–4.

[20] J. Osth, Owais, M. Karlsson, A. Serban, S. Gong, and P. Karlsson, "Direct carrier six-port modulator using a technique to suppress carrier leakage," *IEEE Transactions on Microwave Theory and Techniques*, vol. 59, no. 3, pp. 741–747, 2011.

[21] J. Osth, A. Serban, O. Owais, M. Karlsson, S. Gong, J. Haartsen, and P. Karlsson, "Six-port gigabit demodulator," *IEEE Transactions on Microwave Theory and Techniques*, vol. 59, no. 1, pp. 125–131, 2011.

[22] J.-C. Schiel, S. O. Tatu, K. Wu, and G. Bosisio, "Six-port direct digital receiver (spdr) and standard direct receiver (sdr) results for qpsk modulation at high speeds," in *Proc. IEEE MTT-S Int. Microwave Symp. Digest*, vol. 2, 2002, pp. 931–934.

[23] A. Serban, J. Osth, Owais, M. Karlsson, S. Gong, J. Haartsen, and P. Karlsson, "Six-port transceiver for 6-9 ghz ultrawideband systems," *Microwave and Optical Technology Letters*, vol. 52, no. 3, pp. 740–746, 2010. [Online]. Available: http://dx.doi.org/10.1002/mop.25021

[24] S. O. Tatu, E. Moldovan, K. Wu, and R. G. Bosisio, "A new direct millimeter-wave six-port receiver," *IEEE Transactions on Microwave Theory and Techniques*, vol. 49, no. 12, pp. 2517–2522, 2001.

[25] X. Z. Xiong and V. F. Fusco, "Wideband 0.9 ghz to 5 ghz six-port and its application as digital modulation receiver," *IEE Proceedings - Microwaves, Antennas and Propagation*, vol. 150, no. 4, pp. 301–307, 2003.

[26] X. Xu, R. G. Bosisio, and K. Wu, "Analysis and implementation of six-port software-defined radio receiver platform," *IEEE Transactions on Microwave Theory and Techniques*, vol. 54, no. 7, pp. 2937–2943, 2006.

[27] J. Osth, O. Owais, M. Karlsson, A. Serban, and S. Gong, "Schottky diode as high-speed variable impedance load in six-port modulators," in *Proc. IEEE Int Ultra-Wideband (ICUWB) Conf*, 2011, pp. 68–71.

[28] ——, "Performance evaluation of six-port receivers with simplified interface to amplifier and filter," in *Proc. IEEE Int Ultra-Wideband (ICUWB) Conf*, 2011, pp. 190–194.

[29] W. Ciccognani, M. Ferrari, F. Giannini, and E. Limiti, "A novel broadband mmic vector modulator for v-band applications," *Int. J. RF Microw. Comput.-Aided Eng.*, vol. 20, pp. 103–113, January 2010. [Online]. Available: http://portal.acm.org/citation.cfm?id=1687193.1687201

[30] D. S. McPherson and S. Lucyszyn, "Vector modulator for w-band software radar techniques," *IEEE Transactions on Microwave Theory and Techniques*, vol. 49, no. 8, pp. 1451–1461, 2001.

[31] A. Loke and F. Ali, "Direct conversion radio for digital mobile phones-design issues, status, and trends," *IEEE Transactions on Microwave Theory and Techniques*, vol. 50, no. 11, pp. 2422–2435, 2002.

[32] G. Brenna, D. Tschopp, J. Rogin, I. Kouchev, and Q. Huang, "A 2-ghz carrier leakage calibrated direct-conversion wcdma transmitter in 0.13-um cmos," *IEEE Journal of Solid-State Circuits*, vol. 39, no. 8, pp. 1253–1262, 2004.

[33] A. E. Ashtiani, S.-I. Nam, A. d'Espona, S. Lucyszyn, and I. D. Robertson, "Direct multilevel carrier modulation using millimeter-wave balanced vector modulators," *IEEE Transactions on Microwave Theory and Techniques*, vol. 46, no. 12, pp. 2611–2619, 1998.

[34] B. Razavi, "Design considerations for direct-conversion receivers," *IEEE Transactions on Circuits and Systems—Part II: Analog and Digital Signal Processing*, vol. 44, no. 6, pp. 428–435, 1997.

[35] Y. Xu and R. G. Bosisio, "Effects of local oscillator leakage in digital millimetric six-port receivers (sprs)," *Microwave and Optical Technology Letters*, vol. 19, no. 1, pp. 27–34, 1998. [Online]. Available: http://dx.doi.org/10.1002/(SICI)1098-2760(199809)19:1<27::AID-MOP7>3.0.CO;2-J

[36] I. Elahi, K. Muhammad, and P. T. Balsara, "Iip2 and dc offsets in the presence of leakage at lo frequency," *IEEE Transactions on Circuits and Systems—Part II: Express Briefs*, vol. 53, no. 8, pp. 647–651, 2006.

[37] M. Mohajer, A. Mohammadi, and A. Abdipour, "Direct conversion receivers using multiport structures for software-defined radio systems," *IET Microwaves, Antennas & Propagation*, vol. 1, no. 2, pp. 363–372, 2007.

[38] E. E. Djoumessi, S. O. Tatu, and K. Wu, "Frequency-agile dual-band direct conversion receiver for cognitive radio systems," *IEEE Transactions on Microwave Theory and Techniques*, vol. 58, no. 1, pp. 87–94, 2010.

[39] S. O. Tatu, E. Moldovan, G. Brehm, K. Wu, and R. G. Bosisio, "Ka-band direct digital receiver," *IEEE Transactions on Microwave Theory and Techniques*, vol. 50, no. 11, pp. 2436–2442, 2002.

[40] B. Razavi, "Rf transmitter architectures and circuits," in *Proc. Custom Integrated Circuits the IEEE 1999*, 1999, pp. 197–204.

[41] D. S. McPherson, H.-C. Seo, Y.-L. Jing, and S. Lucyszyn, "110 ghz vector modulator for adaptive software-controlled transmitters," *IEEE Microwave and Wireless Components Letters*, vol. 11, no. 1, pp. 16–18, 2001.

[42] M. Chongcheawchamnan, K. S. Ang, D. Kpogla, S. Nam, S. Lucyszyn, and L. D. Robertso, "Low-cost millimeter-wave transmitter using software radio techniques," in *Proc. Microwave Symp. Digest. 2000 IEEE MTT-S Int*, vol. 3, 2000, pp. 1949–1952.

[43] S. Lucyszyn and I. D. Robertson, "Analog reflection topology building blocks for adaptive microwave signal processing applications," *IEEE Transactions on Microwave Theory and Techniques*, vol. 43, no. 3, pp. 601–611, 1995.

[44] E. M. N. Khaddaj Mallat and S. O. Tatu, "Comparative demodulation results for six-port and conventional 60ghz direct conversion receivers," *Progress In Electromagnetics Research, PIER*, vol. 84, pp. 437–449, 2008.

[45] S. Yamada, O. Boric-Lubecke, and V. M. Lubecke, "Cancellation techniques for lo leakage and dc offset in direct conversion systems," in *Proc. IEEE MTT-S Int. Microwave Symp. Digest*, 2008, pp. 1191–1194.

[46] I. Elahi and K. R. Muhammad, "Asymmetric dc offsets and iip2 in the presence of lo leakage in a wireless receiver," in *Proc. IEEE Radio Frequency Integrated Circuits (RFIC) Symp*, 2007, pp. 313–316.

[47] J. Osth, A. Serban, M. Karlsson, and S. Gong, "Carrier leakage suppression and evm dependence on phase shifting network in six-port modulator," in *Proc. Int. Conf. Microwave and Millimeter Wave Technology*, submitted for publication.

[48] Q. Gu, *RF System Design of Transceivers for Wireless Communications*. Secaucus, NJ, USA: Springer-Verlag New York, Inc., 2006.

[49] S. Y. Zheng, W. S. Chan, and K. F. Man, "Broadband phase shifter using loaded transmission line," *IEEE Microwave and Wireless Components Letters*, vol. 20, no. 9, pp. 498–500, 2010.

[50] S. M. Winter, H. J. Ehm, A. Koelpin, and R. Weigel, "Diode power detector dc operating point in six-port communications receivers," in *Proc. European Microwave Conf*, 2007, pp. 795–798.

[51] R. Mirzavand, A. Mohammadi, and F. M. Ghannouchi, "Five-port microwave receiver architectures and applications," *IEEE Communications Magazine*, vol. 48, no. 6, pp. 30–36, 2010.

[52] S. A. Chakra and B. Huyart, "Five-port receiver for high rates 16qam modulation in the ka-band," in *Proc. IEEE Radio and Wireless Conf*, 2004, pp. 119–121.

[53] J. Osth, M. Karlsson, O. Owais, A. Serban, and S. Gong, "Baseband complexity comparison of six-, five-, and four-port receivers," *Microwave and Optical Technology Letters*, vol. 54, no. 6, pp. 1502–1506, 2012. [Online]. Available: http://dx.doi.org/10.1002/mop.26833

[54] J. Osth, A. Serban, M. Karlsson, and S. Gong, "Lo leakage in six-port modulators and demodulators and its suppression techniques," in *Proc. IEEE MTT-S Int. Microwave Symp. Digest (IMS2012)*, to be published.

[55] N. K. Mallat, E. Moldovan, K. Wu, and S. O. Tatu, "Millimeter-wave ultra-wideband six-port receiver using cross-polarized antennas," *EURASIP J. Wirel. Commun. Netw.*, vol. 2009, pp. 25:1–25:7, January 2009. [Online]. Available: http://dx.doi.org/10.1155/2009/508678

[56] S. Gong, M. Karlsson, A. Serban, J. Osth, Owais, J. Haartsen, and P. Karlsson, "Radio architecture for parallel processing of extremely high speed data," in *Proc. IEEE Int. Conf. Ultra-Wideband ICUWB 2009*, 2009, pp. 433–437.

[57] J. Osth, O. , M. Karlsson, A. Serban, and S. Gong, "Data and carrier interleaving in six-port receivers for increased data rate," in *Proc. IEEE Int Ultra-Wideband (ICUWB) Conf*, vol. 1, 2010, pp. 1–4.

[58] *Revision of Part 15 of the Commissions Rules Regarding Ultra-Wideband Transmission Systems, First Report and Order*, Federal Communication Commission (FCC) ET Docket 98-153, Feb. 2002.

[59] G. F. Engen, "A (historical) review of the six-port measurement technique," *IEEE Transactions on Microwave Theory and Techniques*, vol. 45, no. 12, pp. 2414–2417, 1997.

[60] J. Li, R. G. Bosisio, and K. Wu, "Computer and measurement simulation of a new digital receiver operating directly at millimeter-wave frequencies," *IEEE Transactions on Microwave Theory and Techniques*, vol. 43, no. 12, pp. 2766–2772, 1995.

[61] S. O. Tatu, E. Moldovan, K. Wu, R. G. Bosisio, and T. A. Denidni, "Ka-band analog front-end for software-defined direct conversion receiver," *IEEE Transactions on Microwave Theory and Techniques*, vol. 53, no. 9, pp. 2768–2776, 2005.

[62] P. Hakansson, D. Wang, and S. Gong., "An ultra wide-band I/Q demodulator covering from 3.1 to 4.8 GHz," in *Transactions on Electronics and Signal Processing (ISAST)*, 2008, pp. 111 – 116.

[63] N. Seman, M. E. Bialkowski, S. Z. Ibrahim, and A. A. Bakar, "Design of an integrated correlator for application in ultra wideband six-port transceivers," in *Proc. IEEE Antennas and Propagation Society Int. Symp. APSURSI '09*, 2009, pp. 1–4.

[64] E. Djoumessi and K. Wu, "Tunable multi-band direct conversion receiver for cognitive radio systems," *IEEE MTT-S Int. Microw. Symp. Dig.*, pp. 217–220, Jun. 2009.

[65] J. N. Downing, *Fiber Optic Communications*. Cengage Learning, 2005.

[66] S. M. Winter, H. J. Ehm, A. Koelpin, and R. Weigel, "Six-port receiver local oscillator power selection for maximum output snr," in *Proc. IEEE Radio and Wireless Symp*, 2008, pp. 151–154.

[67] D. M. Pozar, *Microwave Engineering*. John Wiley & Sons, Inc, 2004.

[68] S. A. Maas, *Microwave Mixers*. Norwood, MA: Artech House, 1993.

[69] M. Karlsson, P. Hakansson, and S. Gong, "A frequency triplexer for ultra-wideband systems utilizing combined broadside- and edge-coupled filters," *IEEE Transactions on Advanced Packaging*, vol. 31, no. 4, pp. 794–801, 2008.

[70] C. E. Shannon, "Communication in the presence of noise," *Proceedings of the IEEE*, vol. 86, no. 2, pp. 447–457, 1998.

[71] Z. Zhou, S. Yang, and Z. Nie, "A novel broadband printed dipole antenna with low cross-polarization," *IEEE Transactions on Antennas and Propagation*, vol. 55, no. 11, pp. 3091–3093, 2007.

[72] J. J. A. Lempianen, J. K. Laiho-Steffens, and A. F. Wacker, "Experimental results of cross polarization discrimination and signal correlation values for a polarization diversity scheme," in *Proc. IEEE 47th Vehicular Technology Conf.*, vol. 3, 1997, pp. 1498–1502.

[73] K. Haddadi, H. El Aabbaoui, C. Loyez, D. Glay, N. Rolland, and T. Lasri, "Wide-band 0.9 ghz to 4 ghz four-port receiver," in *Proc. 13th IEEE Int. Conf. Electronics, Circuits and Systems ICECS '06*, 2006, pp. 1316–1319.

[74] K. Haddadi, M. M. Wang, C. Loyez, D. Glay, and T. Lasri, "Four-port communication receiver with digital iq-regeneration," *IEEE Microwave and Wireless Components Letters*, vol. 20, no. 1, pp. 58–60, 2010.